



HAL
open science

Three-Dimensional Architecture, Structural Evolution, and Role of Inheritance Controlling Detachment Faulting at a Hyperextended Distal Margin: The Example of the Err Detachment System (SE Switzerland)

M.-e. Epin, G. Manatschal

► **To cite this version:**

M.-e. Epin, G. Manatschal. Three-Dimensional Architecture, Structural Evolution, and Role of Inheritance Controlling Detachment Faulting at a Hyperextended Distal Margin: The Example of the Err Detachment System (SE Switzerland). *Tectonics*, 2018, 10.1029/2018TC005125 . hal-03102512

HAL Id: hal-03102512

<https://hal.science/hal-03102512>

Submitted on 18 Nov 2021

HAL is a multi-disciplinary open access archive for the deposit and dissemination of scientific research documents, whether they are published or not. The documents may come from teaching and research institutions in France or abroad, or from public or private research centers.

L'archive ouverte pluridisciplinaire **HAL**, est destinée au dépôt et à la diffusion de documents scientifiques de niveau recherche, publiés ou non, émanant des établissements d'enseignement et de recherche français ou étrangers, des laboratoires publics ou privés.

Copyright



Tectonics

RESEARCH ARTICLE

10.1029/2018TC005125

Key Points:

- In-sequence detachment fault evolution leading to exhumation of subcontinental mantle
- Magma-poor distal margin architecture controlled by inherited structures

Correspondence to:

M.-E. Epin,
meepin@unistra.fr

Citation:

Epin, M.-E., & Manatschal, G. (2018). Three-dimensional architecture, structural evolution, and role of inheritance controlling detachment faulting at a hyperextended distal margin: The example of the Err detachment system (SE Switzerland). *Tectonics*, 37, 4494–4514. <https://doi.org/10.1029/2018TC005125>

Received 2 MAY 2018

Accepted 18 NOV 2018

Accepted article online 28 NOV 2018

Published online 11 DEC 2018

Three-Dimensional Architecture, Structural Evolution, and Role of Inheritance Controlling Detachment Faulting at a Hyperextended Distal Margin: The Example of the Err Detachment System (SE Switzerland)

M.-E. Epin¹  and G. Manatschal 

¹Institut de Physique du Globe de Strasbourg, UMR 7516, Université de Strasbourg/EOST, CNRS, Strasbourg Cedex, France

Abstract While extensional detachment systems linked to postorogenic or oceanic settings have been described from many places, examples linked to hyperextension and formation of magma-poor rifted margins remain rare. Here we describe one of the best preserved examples of a detachment system that is exposed over 200 km² in the Err nappe in SE Switzerland. Based on existing and new mapping, we realized a new map that enables to describe the 3-D structure of a detachment system and its role in thinning the crust and controlling the architecture and structural evolution of a hyperextended margin. We show that the Err detachment system is formed by at least three in-sequence detachment faults. The 3-D architecture of these faults and of their hanging wall blocks is controlled by inherited structures and a prerift evaporite level. The geometrical relationships and the evolution of the detachment system show deviations from the classical rolling hinge model. From the observations it remains unclear how and where the detachment faults rooted at depth. The overall observations made in the Err nappe allow to describe how the final rift evolution preceding mantle exhumation can be explained by extensional detachment systems and how these structures shape the hyperextended continental wedge at distal margins. While these questions are difficult to answer at present-day rifted margins, the use of a kilometer-scale field analogue can help to upscale and to interpret extensional detachment systems at present-day distal, magma-poor rifted margins.

1. Introduction

Hyperextended rifted margins and associated extensional detachment faults, also referred to as long-offset normal faults, have been investigated and discussed using field and seismic observations (Manatschal, 2004; Reston & McDermott, 2011; Sutra & Manatschal, 2012) and numerical modeling (Brune et al., 2014; Huisman & Beaumont, 2011). However, how these detachment faults form, the angle at which they slip (low versus high angle), and how they evolve (in sequence versus out of sequence) remains debated. A popular model to explain how these faults form is the rolling hinge model, which suggests that these faults form at high angles and rotate near the surface to low angles (e.g., Axen & Bartley, 1997; Buck, 1988; Wernicke & Axen, 1988). This model has been used to describe extensional detachment faults at metamorphic and oceanic core complexes, that is, in settings undergoing postorogenic collapse or at slow to ultraslow spreading systems. In contrast, the processes that explain detachment faults forming in hyperextended domains remain ill constrained, mainly due to the lack of high-resolution seismic imaging and direct observations. One of the best examples of an extensional detachment system formed in a hyperextended domain is exposed in the Err nappe in Grisons in southeastern Switzerland.

The aim of this paper is to discuss the architecture of a detachment system related to hyperextension and crustal thinning. We describe, based on field observations and mapping, the 3-D architecture of the Err detachment system and the type of rocks preserved in their footwall and hanging wall. We restore the 3-D architecture of this detachment system over an area of 225 km² and discuss its tectonic evolution and the role of inheritance, in particular of an inherited Paleozoic basin and of prerift Triassic evaporites in controlling its architecture. Our observations enable to demonstrate that the detachment system consists of at least three faults that formed in sequence. The overall geometrical relationships, in particular the occurrence of allochthonous blocks and the cross-cutting relationships of the single faults, suggest deviations from the classical rolling hinge model that may be explained by inheritance in the pre-extensional layers.

2. Geological Setting and Previous Studies

2.1. Geological and Geographical Overview

The Late Cretaceous Lower Austroalpine and Upper Penninic nappes in SE Switzerland consist of remnants of the fossil Jurassic southwestern distal Adriatic margin that contain fragments of an extensional detachment system (Figure 1a). In this study, we focus on an extensional detachment system that is well preserved and exposed in one of these nappes, which is the Err nappe (Figure 1b). The Err nappe was stacked, together with the overlying Bernina and underlying Platta nappes in an external part of the Eo-Alpine system during onset of convergence in Late Cretaceous time (Figure 1c). This shortening occurred during the closure of the northern Meliata-Vardar domain. Thrusting occurred in a top-to-west fold and thrust belt that initiated in Late Cretaceous. Within the Bernina, Err, and Platta nappes the metamorphic overprint never exceeded lower greenschist facies conditions during Alpine shortening (Ferreiro Mählmann, 1994, 1996). During Eocene to Oligocene south-north directed shortening, structures in the study area were only locally reactivated, which explains the excellent preservation of the Jurassic detachment system. This is due to the fact that the Err nappe was located during the Eocene to Oligocene north-south directed collision in the neutral zone above the singular point, that is, the northernmost tip of the Adriatic buttress (Schmid et al., 1996) separating pro-thrusting and retro thrusting. In the past, the complex rift structures and in particular the lack of continuity of prerift and synrift sedimentary sequences made it difficult to describe and evaluate the Alpine overprint in the Err nappe. Only more recently, Epi et al. (2017) were able to distinguish between pre-Alpine and Alpine structures and to describe the role of rift inheritance during Alpine convergence. This study enabled to recognize and map new parts of an extensional detachment system, from which parts were previously described by Froitzheim and Eberli (1990), Handy et al. (1993), Handy (1996), Froitzheim and Manatschal (1996), Manatschal and Nievergelt (1997), Masini et al. (2011), and Masini and Manatschal (2014), and to demonstrate that the extensional detachment system consists of multiple faults that formed in sequence. Apart from the Err nappe, detachments faults have also been described from the Platta and Bernina nappes. At least five single faults, belonging to a Jurassic extensional detachment system are preserved in these units, extending over more than 600 km². This study will focus on the detachment system exposed in the Err nappe. Since in this nappe three fault branches of an extensional detachment system are exposed in one single thrust sheet, it is possible to describe the geometrical relationships between these single Jurassic faults without the need to make assumptions of the Alpine overprint.

2.2. Historical Discovery

The discovery of extensional detachment systems in the Basin and Range (Davis et al., 1980; Davis & Lister, 1988; John, 1987; John & Foster, 1993; Lister & Davis, 1989; Spencer & Chase, 1989) is at the origin of new models describing extensional systems (e.g., simple shear and rolling hinge models; Buck, 1988; Nagel & Buck, 2007; Spencer, 1984; Wernicke, 1985; Wernicke & Axen, 1988). Although, at present, extensional detachment faults are common and described from different extensional regimes, ranging from late to postorogenic to slow and ultraslow spreading ridges (see John & Cheadle, 2010 and Whitney et al., 2013, for reviews), examples related to the formation of hyperextended margins are rare. This is due to the difficulty to access these structures in a present-day margin, where they are commonly overlain by kilometers of sediments and water. Boillot et al. (1987), proposed a detachment fault model for the Iberia rifted margin in order to explain the occurrence of subcontinental mantle rocks at the seafloor (Ocean Drilling Program, Leg 103, Boillot et al., 1988). At the same time, Lemoine et al. (1987) proposed a simple shear detachment model for the formation of the Alpine Tethys rifted margins. The first descriptions and interpretations of preserved and exposed extensional detachment faults in the Alps were made by Froitzheim and Eberli (1990), Florineth and Froitzheim (1994), Froitzheim and Manatschal (1996), and Manatschal and Nievergelt (1997). These rift-related detachment faults are located in the Err and Tasna nappes in SE Switzerland. They are formed by tens of meter thick damage zones constituted of characteristic green fault rocks (cataclasites) and a core zone made of black indurated fault gouges showing a specific geochemical signature (Incerpi et al., 2017; Manatschal et al., 2000; Picazo et al., 2013; Pinto et al., 2013, 2015). Masini et al. (2012) investigated the tectono-sedimentary evolution of the detachment system in the Err unit (e.g., Samedan basin; Masini et al., 2011). Although at present the occurrence of extensional detachment systems is well accepted and the examples in the Alps well documented, the 3-D architecture and structural evolution of these fault systems are still debated as well as the role of inheritance in shaping the final architecture of these fault systems.

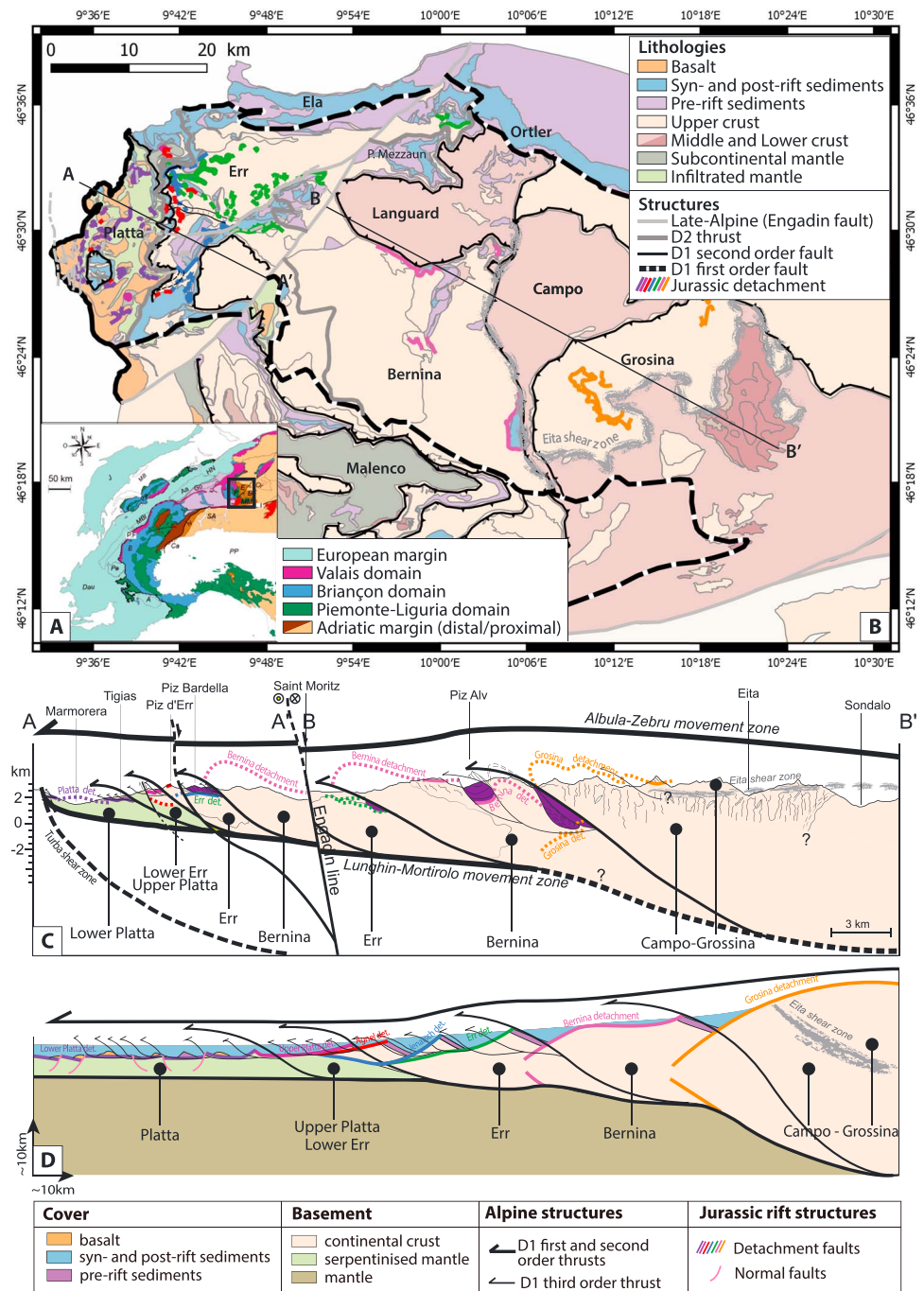


Figure 1. (a) Tectonic overview map of the Alps (Mohn et al., 2011, modified after Schmid et al., 2004). (b) Geological map of the Austroalpine and Upper Penninic nappes in SE Switzerland and north Italy. Map modified after a compilation of Mohn et al. (2011). (c) Present-day Alpine section across the Upper Penninic and Austroalpine nappes (modified after Mohn et al., 2011). (d) Architecture of the Adriatic margin based on the restoration of the Austroalpine nappe system, with the location of future first, second and third-order D1 thrusts (modified after Epin et al., 2017).

2.3. Pre-Alpine and Alpine Structures

The recognition and study of precollisional rift-related structures in the Alpine belt became possible because of its long and detailed geological description. Pioneering work by several generations of geologists including Steinmann (1925), Elter (1972), Bernoulli (1964), Lemoine et al. (1987), Lagabrielle and Cannat (1990), Frotzheim and Eberli (1990), and many others enabled to define pre-Alpine rift-related structures within

the Alpine mountain belt. Although the control of the rift inheritance has been proposed by many authors (Beltrando et al., 2014; Butler, 1989; Butler et al., 2006; Handy, 1996; Handy et al., 1993; Mohn et al., 2014), the details of the interaction between inherited structures and their reactivation are still debated and little understood. Epin et al. (2017) presented, using the example of the Err and Platta nappes, a detailed analysis of the role of rift inheritance during reactivation of a hyperextended and exhumed rift domain. This study builds on the work of Epin et al. (2017) and previous studies, in which the main Alpine and pre-Alpine structures in the Err nappe have been described (see Figures 1–7, Epin et al., 2017). The main Alpine structures and deformation phases can be described as follows:

1. The D1 phase (e.g., Trupchun phase of Froitzheim et al., 1994) is related to the major, top-to-west Alpine shortening manifested by the emplacement of the Austroalpine nappe stack during Late Cretaceous convergence (Froitzheim et al., 1994). In the study area, this phase is responsible for the sandwiching of the Err nappe between the underlying Platta nappe (exhumed mantle and proto-oceanic crust) and the overlying Bernina nappe (hyperextended continental crust) along major D1 thrust faults (black dotted fault, Figure 1). Second-order D1 thrusts (black thin fault, Figure 1) subdivide the Err nappe in the Upper, Middle, and Lower Err units (for more details, see Manatschal & Nievergelt, 1997; Epin et al., 2017).
2. The D2 phase (e.g., Ducan-Ela phase of Froitzheim et al., 1994) is mainly expressed by normal faults (gray fault, Figure 1) reactivating and/or crosscutting older D1 structures (e.g., Handy et al., 1993; Manatschal & Nievergelt, 1997).
3. The D3 phase (e.g., Blaisun phase of Froitzheim et al., 1994) affected the Err nappe by north and south directed thrust splays and kilometer-scale (not representing on the map, Figure 1), upright east west striking open folds.
4. The D4 and D5 phases of Froitzheim et al. (1994) are manifested in the study area by late east-west directed high-angle faults (light gray fault, Figure 1) already mapped by Cornelius (1932). Handy (1996) suggested that these faults are related to the Engadin fault that postdate the Bergell intrusion (30myr).

The hanging wall of the Tertiary Alpine subduction zone is only slightly deformed, which explains why the rift-related structures in the Err nappe are so well preserved (Cornelius, 1932; Froitzheim et al., 1994; Handy, 1996; Handy et al., 1993, 1996; Manatschal & Bernoulli, 1999; Manatschal & Nievergelt, 1997; Masini et al., 2011, 2012; Stöcklin, 1949). In this paper we show that the Jurassic, rift-related extensional detachment system consists of at least three fault branches that formed by in-sequence faulting. Although previous studies recognized the existence of two detachment faults (e.g., Err and Jenatsch detachments of Manatschal, 1999; Masini et al., 2012; Manatschal et al., 2015), the way they interacted during extension remained unclear in the previous studies.

3. Extensional Detachment Systems in Hyperextended Rifted Margins

3.1. Extensional Detachment Systems

Rift models explaining crustal thinning and mantle exhumation often include extensional detachment systems. The Iberia and Galicia margins are at present the best documented magma-poor rifted margins, where hyperextension and mantle exhumation have been proven by drill hole data. Fossil analogues are the Alpine Tethys margins, where remnants of the former distal margin including hyperextended crust and exhumed mantle are exposed. These examples, supported by dynamic modeling, show that final extension at magma-poor rifted margins is accommodated along extensional detachment faults (Duretz et al., 2016; Manatschal et al., 2001; Perez-Gussinye & Reston, 2001; Péron-Pinvidic & Manatschal, 2010). When the crust is thinned to less than 10 km, first faults can penetrate the subcontinental mantle and lead to its exhumation at the seafloor (Manatschal, 2004; Perez-Gussinye & Reston, 2001; Péron-Pinvidic et al., 2007; Reston et al., 2004). How the different detachments evolve and progressively thin and exhume the crust during final rifting remains yet unclear.

3.2. Characteristics of the Err Detachment System

The Err detachment system is formed by a brittle damage zone that is made of characteristic fault rocks including green cataclasites and black indurated gouges (Manatschal, 1999; Pinto et al., 2013, 2015). Manatschal and Nievergelt (1997) and Masini et al. (2012) mapped the detachment in the Err nappe and studied the structures and kinematics of the detachment system in the area between Piz Err and Piz Bial in

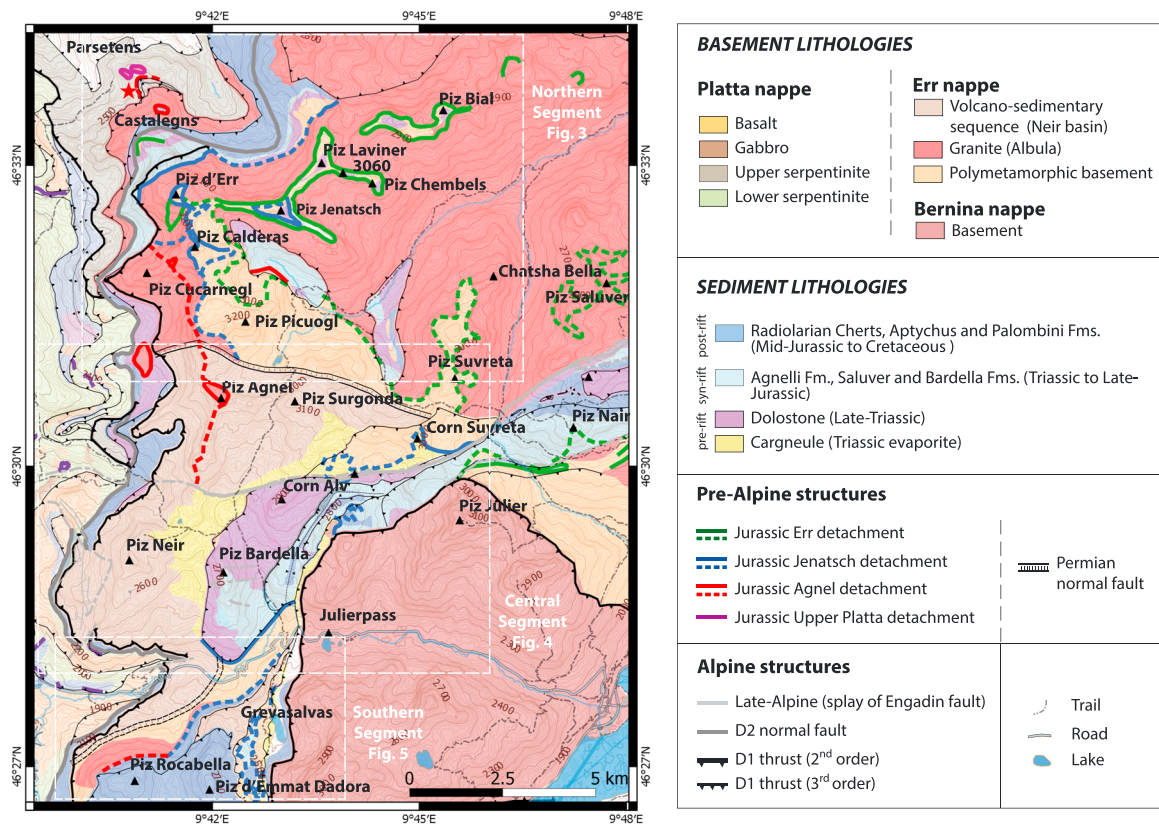


Figure 2. Tectonic map of the Err nappe showing the location of the different Jurassic detachment faults and Alpine thrusts (based on new observations and a compilation of previous maps; for reference see Masini et al., 2011; Epin et al., 2017).

the north and Piz Nair and Piz Bardella in the south of the Err nappe (see Figure 2 for locations). Based on the analysis of *s-c* fabrics, shear bands and sigma clasts within the indurated gouges, a top-to-west transport direction was determined (Froitzheim & Eberli, 1990; Manatschal & Nievergelt, 1997). The detachment system separates hanging wall blocks from a massive and continuous footwall. Locally, Triassic prerift evaporites occur along the detachment faults. Their importance and role during the formation of the extensional detachment system, as well as the occurrence of a Permian basin will be discussed in this paper.

3.3. Geometry of the Detachment Fault and Relation to Basement Rocks and Sediments

Former studies discussed mainly the 2-D rift structures along E-W striking dip lines, that is, parallel to the transport direction across the area between Piz Err and Piz Bial (e.g., northern segment in Figures 2 and 3; Manatschal & Nievergelt, 1997; Masini et al., 2012). In these sections (Figure 3e) two extensional detachment faults, the Err and Jenatsch detachment faults, were identified and mapped. However, the relationship between these two detachment faults remained unclear. North-south striking sections perpendicular to the transport direction, that is, a strike line, have been published in Masini et al. (2012) and Manatschal et al. (2015). These north-south sections (see Figure 7 in Manatschal et al., 2015) show a very complex geometry, interpreted as a lateral ramp of a detachment fault that was controlled by the existence of a Permian basin, referred to as the Neir basin (Manatschal et al., 2015). This complexity made it difficult to correlate the well-exposed detachment faults in the north with remnants of exposed detachment faults in the south (Bardella and Grevasalvas area Figure 2). This is mainly due to the change in composition of the footwall from mainly Carboniferous granites intrusive into polymetamorphic Paleozoic gneisses and schists in the north to volcano-sedimentary sequences belonging to a Permian basin in the south. The volcano-sedimentary series are characterized by porphyritic rhyolites interleaved with volcano-clastic sequences that grade upward into subareal sandstones and conglomerates belonging to the Chazforà and Fuorn formations (Fms.; Doessegger, 1974). The Permian extensional to transtensional structures resulted in a strong and, for

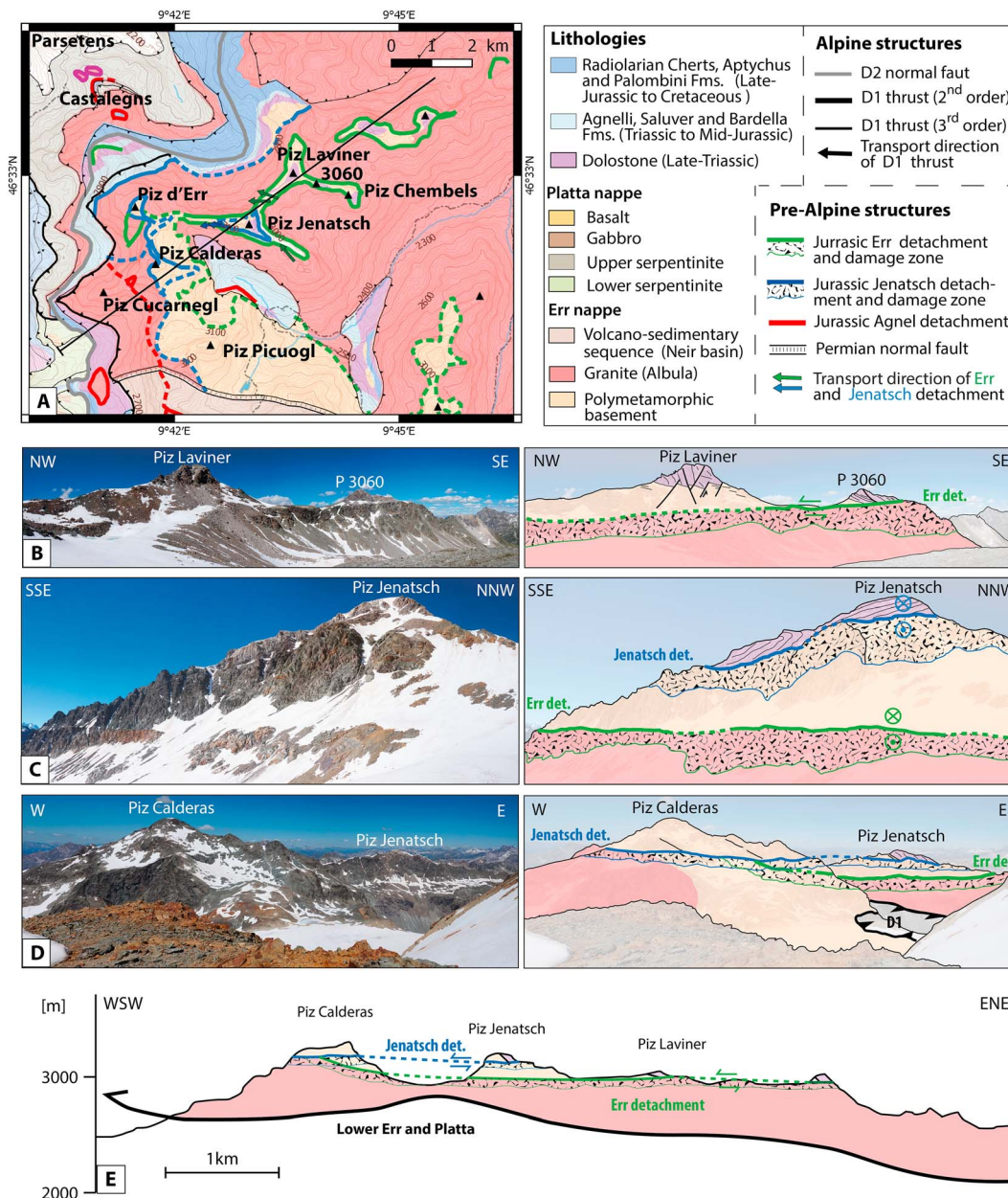
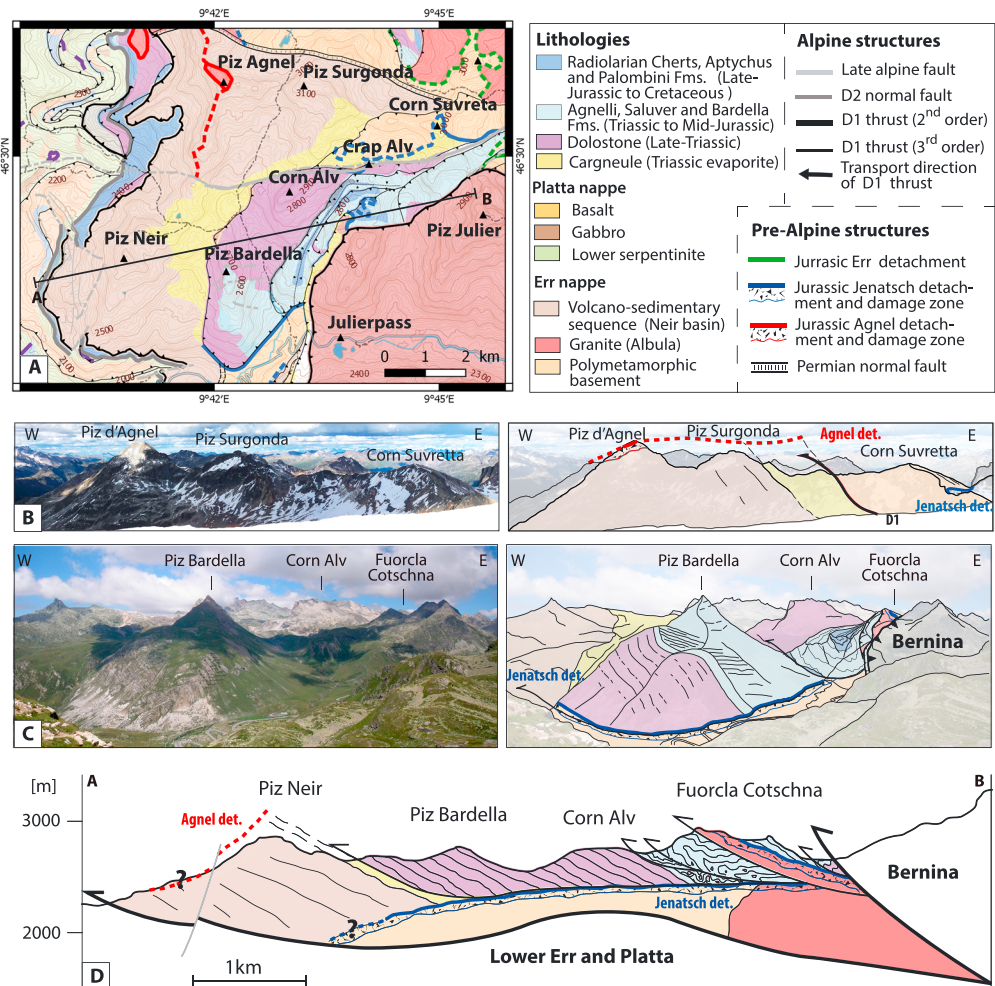


Figure 3. Tectonic map and sections through the northern segment. (a) Tectonic and structural map of the northern segment. (b) Panoramic view of the Piz Laviner and P 3060 showing the Err detachment fault. (c) Panoramic view of the Piz Jenatsch showing the Jenatsch and Err detachment faults (view in transport direction). (d) Panoramic view of Piz Calderas and Piz Jenatsch showing the Jenatsch detachment truncating the Err detachment. (e) Section parallel to transport direction across the northern segment of the Err nappe.

the subsequent rift evolution, important inheritance that will be discussed in this paper. Another important observation is the occurrence of Triassic evaporites that are locally found along the detachment system and at the base of extensional allochthonous blocks. Detailed mapping of the along-strike changes described in the next chapter enables to better constrain the lateral continuity of the different branches of the detachment system, referred to as the Err, Jenatsch, Agnel, and Upper Platta detachment faults.

The *hanging wall*, hereafter defined as consisting of all sequences that structurally and/or depositionally overlie the extensional detachment faults, is made of upper-crustal rocks and prerift to postrift sediments and, on the most distal parts (Platta nappe), also of synextensional magmatic additions. As discussed in this paper, the middle Triassic evaporites had an important control on the structural development of the hanging wall. This



is indicated by the fact that within the hanging wall, preevaporite and postevaporite sequences are never observed within one continuous sequence, suggesting that the evaporate level was used as a decoupling level during extension. Another important point discussed in this paper is the lateral termination of the extensional allochthons and its implication for the 3-D geometry of the extensional detachment system.

In order to understand the timing of the creation of accommodation space and the subsidence history and related depositional environments, it is critical to link the sedimentary evolution to that of the extensional detachment faults. The synextensional sediments can be subdivided into the Agnelli, the Bardella, and the Saluver Fms. (for more details see Masini et al., 2011). These formations (Fms.) are predetachment to postdetachment faulting, despite the fact that at the scale of the entire margin, they formed during rifting, that is, belong to the synrift sequence (e.g., Masini et al., 2013). Based on the detailed relationship between the detachment system and the synrift sediments, Masini et al. (2012) suggested a migration of deformation toward the future ocean. Moreover, the depositional environments also show a deepening of the distal margin during its formation (e.g., Decarlis et al., 2015). The Agnelli Fm. that is predetachment faulting shows a platform environment, suggesting a shallow bathymetry at onset of detachment faulting. The syndetachment sediments, the Bardella and the Saluver Fms., are made of breccias, turbidites, and hemipelagic sediments that show a deepening of the future distal margin, which is consistent with the occurrence of deep

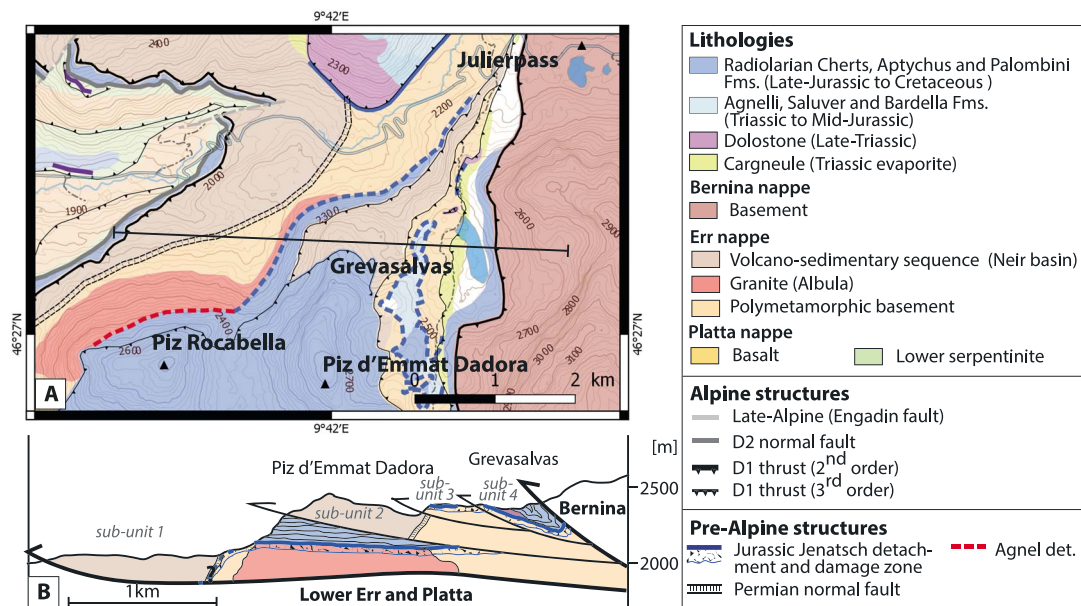


Figure 5. Tectonic map and section through the southern segment. (a) Tectonic and structural map of the southern segment. (b) Section in transport direction (Jurassic and Alpine D1) across the southern segment separated in 4 Alpine subunit.

marine sediments depositionally downlapping/onlapping onto detachment faults. Based on geometrical relationships between sediments and detachment faults, maximum and minimum ages of the detachment system can be determined. A maximum age for the onset of detachment faulting is 187 Ma (Early Pliensbachian), which corresponds to a hardground capping the Agnelli Fm (Dommergues et al., 2012). This hard ground is truncated by the Jenatsch detachment fault, indicating that the Jenatsch detachment has to be younger. A minimum age for the detachment system in the Err nappe is the Bathonian-Callovian Radiolarian chert Fm. (Bill et al., 2001), which is the first formation that depositionally overlies the basalts with a Mid Oceanic Ridge signature deposited over mantle rocks in the Platta nappe. As we will discuss later, the lateral distribution of these syntectonic to posttectonic sediments is complex and their deposition is intimately related to the 3-D evolution of the extensional detachment system. The observation that locally synrift sediments depositionally overlie at a low angle exhumed detachment faults is in line with the interpretation that these detachment faults were locally exhumed and were at a low angle ($<15^\circ$) when they reached the seafloor. However, the occurrence of postrift sediments depositionally overlying detachment faults (e.g., Roccabella; southern Err nappe) also shows that their 3-D structure was complex and had to include lows and highs. In this paper we will discuss the morphotectonic evolution and final 3-D architecture of the Err detachment system.

4. Three-Dimensional Architecture of the Extensional Detachment System Exposed in the Middle Err Unit

In this chapter we present the key observations made in the field and shown in the maps and in the sections (Figures 2–7 and summarized in Figure 8). We subdivide the study area in three segments, a northern, a central, and a southern one and describe E-W and N-S trending sections corresponding to dip and strike sections. Each of the segments preserves different relations between footwall and hanging wall rocks and inherited structures. The northern segment is located along the mountain ridge formed by Piz d'Err, Piz Calderas, Piz Jenatsch, Piz Laviner, and Piz Bial. The central segment is located around Piz d'Agnel, Piz Bardella, and the Fuorcla Cotschna area, and the southern segment is located at the south of the Julier road around Grevasalvas, Piz d'Emmat Dadora, and Piz Rocabella (Figure 2). It is important to note that all segments are in one and the same Alpine tectonic unit, which is the Middle Err unit (Manatschal & Nievergelt, 1997). As a consequence, the Alpine overprint is negligible in the north and moderate in the south and the pre-Alpine structures can be restored with confidence.

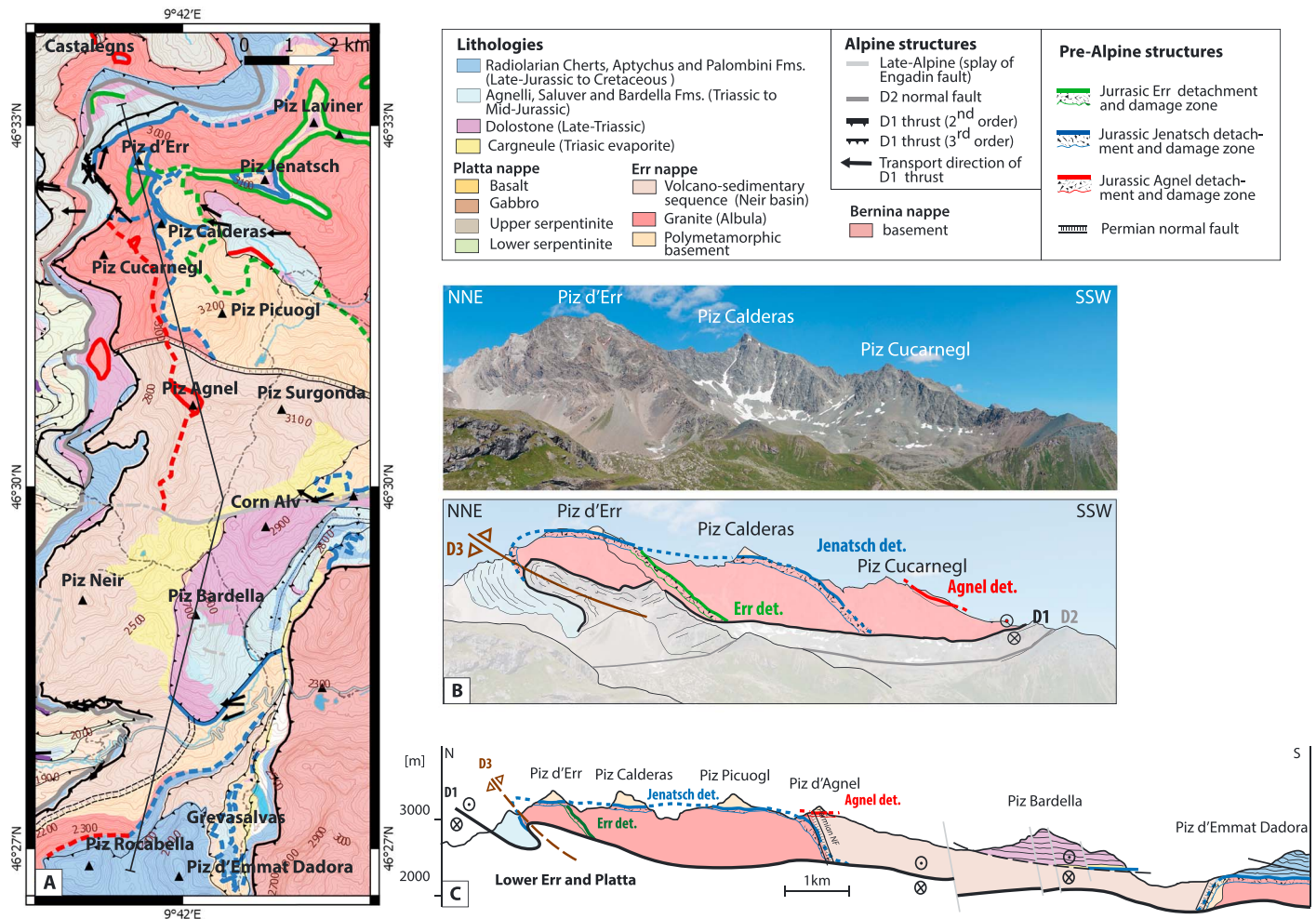


Figure 6. Tectonic map and N-S strike section perpendicular to the Jurassic and main Alpine (D1) transport direction. (a) Tectonic and structural map of the western Err nappe. (b) Panoramic view of the Piz d'Err and Piz Calderas area showing lateral variations of the detachment geometry. (c) N-S section showing the lateral ramps of the Jenatsch detachment controlled by the presence of the Permian basin.

4.1. The Northern Segment

In the northern segment (Figure 3), between Piz d'Err and Piz Bial, the detachment system is best exposed. This area corresponds also to the location where the Err detachment system has been first described (Froitzheim & Eberli, 1990). Detailed mapping enables to follow the detachment system over 200 km². It is important to note that the relation between the rift-related detachment faults and the Alpine D1 thrust fault, forming the base of the Middle Err unit (Manatschal & Nievergelt, 1997), can be mapped in 3-D (Figure 3a). The intersection between the two structures is E-W directed, that is, parallel to the sense of shear in the two structures. In the area of Piz Jenatsch and Piz Calderas (Figure 3), two detachment faults are observed. These detachment faults have been described previously and referred to as the Err and Jenatsch detachments faults (Manatschal & Nievergelt, 1997).

The Err detachment fault (green line, Figure 3) is well exposed in the area of Piz Bial and Piz Laviner. It is characterized by a footwall that is made of a massive granitic basement (Albula Granite) that becomes more deformed and cemented by silica toward its top, that is, the detachment surface. In sections perpendicular to the detachment, one can see a gradual transition from massive granites to green, silica-rich cataclasites with sharp contacts to black, indurated gouges that define the detachment surface. The transition can occur through hundreds of meters and can also be, locally, less than 50 m.

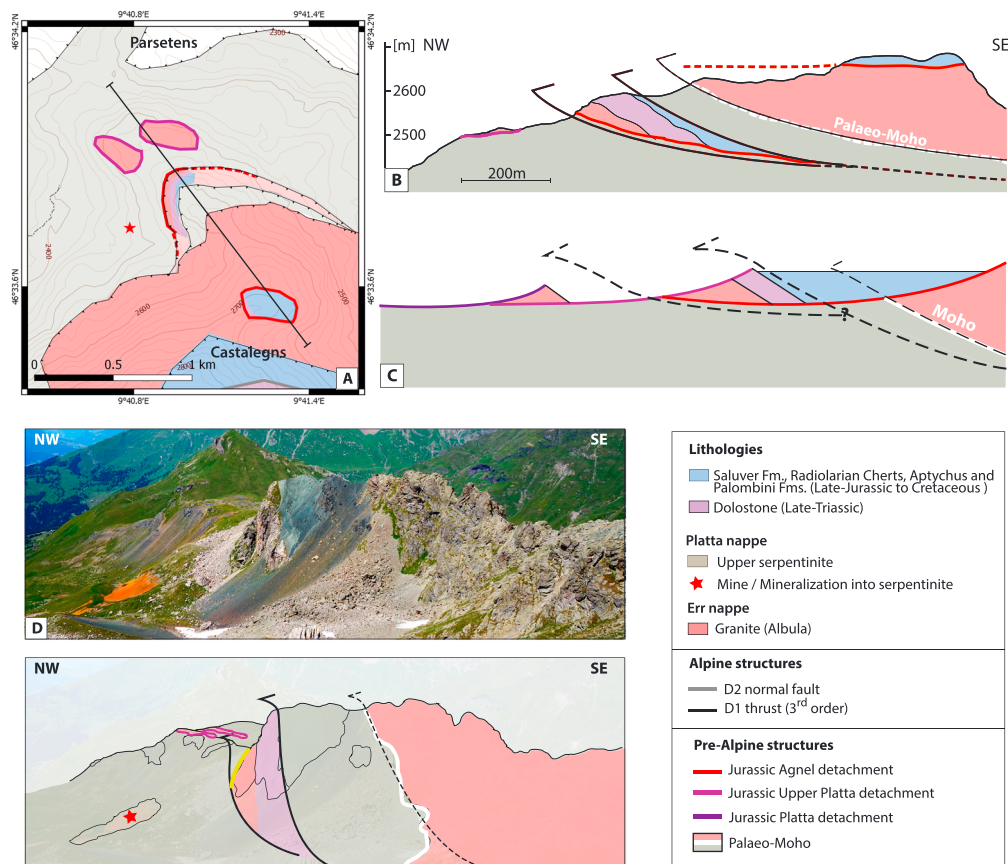


Figure 7. Tectonic map and section of the northeastern part of the Err nappe corresponding to the Lower Err and Upper Platta units. (a) Tectonic map of the northern Castalegns-Parsetens area. (b) Section through the northern Castalegns-Parsetens area. (c) Schematic restoration of the Castalegns area showing the occurrence of allochthonous blocks of continental basement onto exhumed subcontinental mantle. (d) Panoramic view of the northern Castalegns-Parsetens area.

The hanging wall of the Err detachment fault is made of gneisses and schists belonging to the polymetamorphic Variscan basement. Since these rocks preserve primary contacts to Permian extrusive rocks elsewhere and can be found reworked in Permian sediments, these rocks had to be in the upper crust before detachment faulting started. The contact between the basement and the overlying Permian to Lower Jurassic prerift sediments is complex and will be described below. The stratigraphic successions are often thinned and incomplete; however, stratigraphic repetitions are never observed. Detailed observations show that the sedimentary successions are affected by polyphase normal faulting that affect in particular the Triassic evaporites. Locally, as for instance at Piz Lavinèr, normal faults (pink fault, Figure 3b) are associated with the formation of neptunian dykes filled with the surrounding material in the presence of a calcareous sedimentary matrix. This suggests that the hanging wall underwent extension near or at the seafloor, before being uncomfortably overlain by mid Jurassic to lower Cretaceous synrift to postrift sediments (Manatschal & Nievergelt, 1997). Along the mountain ridge between Piz Lavinèr and Piz d'Alp Val and Piz Bial, both tilting to the east and to the west can be observed in the hanging wall blocks. It is important to note that the faults that accommodate the tilting are truncated by the Err detachment fault, with the exception of one fault, which is east of P.3060. This structure truncates the detachment fault. At Piz Jenatsch, the younging of the sedimentary sequence indicates an east-side-down tilting of the hanging wall (Figure 3). Between Piz Lavinèr and Piz Bial, tilting of the blocks is more complex and occurs in different directions. Kinematic and structural analyses show a top-to-west transport direction (Froitzheim & Eberli, 1990; Manatschal & Nievergelt, 1997). The intersections between stratigraphic layers in the Triassic dolostones and high-angle normal faults strike predominantly SW-NE, indicating that they are oblique to the movement direction documented along the detachment fault, which is E-W directed

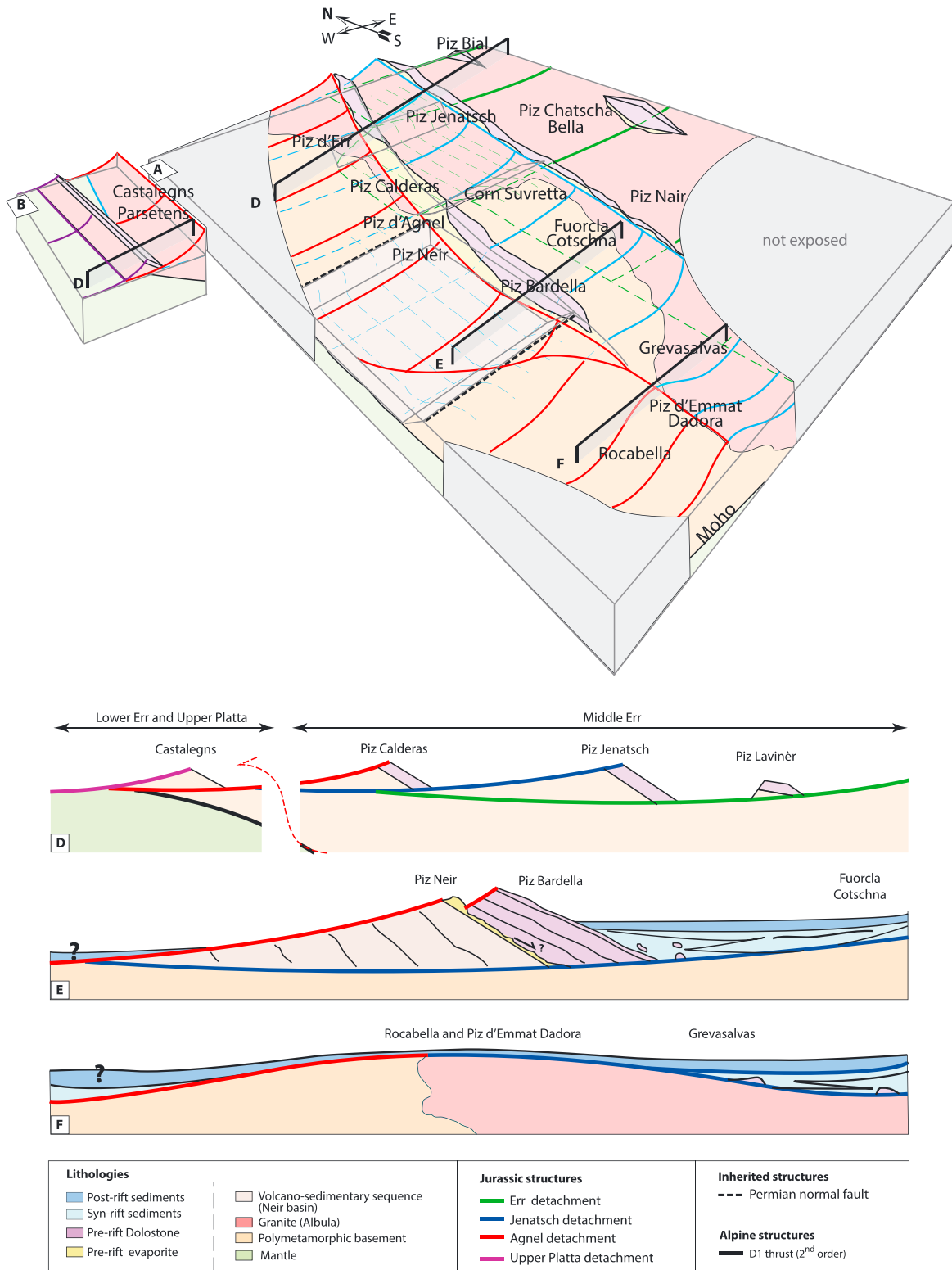


Figure 8. Restoration of the Err nappe. (a) Restored block of the Err nappe showing the location of different detachment faults. (b) Restored block of the Lower Err and Upper Platta unit showing the transition from the hyperextended domain to the exhumed mantle domain. (c) Schematic map of the Err domain showing distribution of detachment faults and the lateral termination of allochthonous blocks. (d) Simplified restored section through the northern Err and Upper Platta domains. (e) Simplified restored section through the southern segment. (f) Simplified restored section through the southern segment.

(see compiled transport directions in Figure 3a; Manatschal & Nievergelt, 1997; Masini et al., 2012, and own observations).

The Jenatsch detachment fault (blue line, Figure 3) is well exposed at Piz Jenatsch and Piz Calderas. At Piz Jenatsch, the footwall of the Jenatsch detachment corresponds to the hanging wall of the Err detachment. It contains a characteristic, reddish K-feldspar bearing granite, with phenocrysts up to 4-cm long (Manatschal & Nievergelt, 1997). At Piz Calderas, the footwall of the Jenatsch detachment is composed of granite and gneiss showing intrusive contacts of the former into the latter. Similar to the Err detachment, the basement shows a strong cataclastic overprint that becomes more pronounced toward the detachment surface. The hanging wall of the Jenatsch detachment at Piz Jenatsch is made of a gneissic basement that is overlain along a stratigraphic contact by Permo-Triassic sediments. The bedding of this sequence forms a low angle (between 15° and 45°) with the detachment surface and dips to the east to southeast. The sediments at Piz Jenatsch are, however, cross cut by several normal faults, some of which are subparallel to bedding and some are steeply dipping with a NE-SW trending direction. At Piz Calderas, the hanging wall of the Jenatsch detachment is made of gneiss. The dipping of the foliation in the gneiss is east to southeast, similar to the one observed at the top of Piz Jenatsch.

Since the intersection of the two detachment faults, obscured by the strong cataclastic overprint, was not clearly mapped in the past, the relationship between the two detachment faults remained unclear. A detailed mapping of the area between Piz Agnel, Piz Jenatsch, and Piz Err enabled to show that the Err detachment is intersected by the Jenatsch detachment (Manatschal and Nievergelt, 1997, suggested the opposite). Moreover, the new mapping also enabled to identify and map a new detachment surface, referred to as the Agnel detachment (for details see below). In the panoramic views shown in Figure 3c, and the section shown in Figure 3d, the cross-cutting relation between the Err and the Jenatsch detachment faults is shown. In the area of Piz Laviner and further east, only the Err detachment fault is present and overlain by small allochthon constituted of basement and prerift sediments. At Piz Jenatsch, it can be observed that the Jenatsch detachment occurs in the hanging wall of the Err detachment. Further south, at Piz Calderas, it can be observed that the Err detachment is indeed overprinted by the cataclastic damage zone belonging to the footwall of the Jenatsch detachment. Detailed mapping allows to follow the Jenatsch detachment westward toward Piz d'Err, where it intersects the underlying Err detachment. The cross-cutting relationships can be best observed in an east-west trending section (Figure 3e), indicating that the two structures intersected at an angle of about 20° to 30°.

4.2. The Central Segment

In the central segment of the Err unit, in the area of Piz Neir, Piz d'Agnel, Piz Bardella, and Piz Surgonda (Figure 4), the rift structures were partly reactivated during Alpine convergence. However, this reactivation is minor and displacements are in the order of <1 km, as indicated by the mapping of cut off points.

In the central segment, two detachment faults are identified: the Jenatsch detachment (blue line, Figure 4) and the Agnel detachment (red line, Figure 4). Previous studies suggested that Piz Bardella, the western Samedan basin including the Fuorcla Cotschna area, were underlain by the Err detachment (Masini et al., 2012). However, detailed mapping shows that the detachment underlying these areas corresponds to the Jenatsch detachment (blue line, Figure 4). The north-south correlation between these detachment faults and between the different segments will be discussed in section 4.4.

At Piz d'Agnel (Figure 4b), which lies in the hanging wall of the Jenatsch detachment, another detachment surface, referred to as the Agnel detachment, can be observed. It can be identified by the occurrence of characteristic silica-rich green cataclasites. The hanging wall of the Agnel detachment is only exposed at Piz Agnel and is made of gneissic basement. The footwall of the Agnel detachment consists of a thick Permian volcano-sedimentary sequence that is well exposed south of Piz d'Agnel and Piz Surgonda at Piz Neir. Further north, the basement is made of granite and gneiss. As shown on the map (Figure 4), the Agnel detachment (red line) truncates the east-west striking contact separating the thick Permian volcano-sedimentary sequence in the south from the granitic and gneissic basement to the north. This contact corresponds, as discussed later, to an inherited, east-west striking Permian normal fault that controls the local architecture of the Jurassic detachment fault (see section 4.4). On the panoramic view shown in Figure 4b, we can see that the footwall, made of a Permo-Triassic volcano-sedimentary sequence, is the more steeply tilted of the area with an angle between 30° and 50° to the east.

The top of the Piz Neir is the lateral continuity of the Piz d'Agnel-Piz Surgonda tilted block. It is therefore interpreted as a part of the footwall of the Agnel detachment. The detachment is not preserved, due to erosion.

In the panoramic view shown in Figure 4c (view perpendicular to the transport direction), it can be seen that the Bardella block is tilted eastward and truncated at the base by the Jenatsch detachment fault. The base of the Triassic dolostones at Piz Bardella is made of cargneules (reworked dolostones with evaporites). The cargneules can be mapped toward Piz Neir separating the massive Permian volcano-sedimentary sequence in its footwall from the dolostones forming the Bardella block. The layering within this sequence shows a general tilting to the east with an angle of 30°–48°, similar to what can be observed in the area of Piz Surgonda. As a consequence, the Bardella block lies also in the footwall of the Agnel detachment and is floored by the Jenatsch detachment. The occurrence of cargneules (i.e., Triassic evaporites) at the base of the Bardella block played, as discussed below, an important role during extension and subsequent convergence.

The area between Piz Bardella and the Fuorcla Cotschna area is affected by third-order D1 thrusts with displacements of hundreds of meters that have been accommodated along thrust faults that are mapped and discussed in Epin et al. (2017). In their reconstruction, the eastward continuation of the Jenatsch detachment flooring the Bardella block can be found at the Fuorcla Cotschna area (Figure 4c), where it separates strongly deformed basement rocks in the footwall from Jurassic synrift sediments in the hanging wall (Handy et al., 1993; Manatschal & Nievergelt, 1997; Masini et al., 2012). The detachment surface is made of green cataclasites that are transected by anastomosing black indurated gouges. The Jurassic synrift sediments are made of sandstones belonging to the Bardella and Saluver Fms. (Finger, 1978) that unconformably overlie the Jenatsch detachment fault with an angle of 20°–30°. The Bardella and Saluver Fms. show an evolution from bottom to top (for more detail see Masini et al., 2011) initiating with breccias made mostly of basement clasts, interleaved with black claystones showing a similar chemical composition to the black indurated gouges (Manatschal, 1995). These breccias grade up section into sandstones that are interleaved with carbonate-rich breccias and olistoliths. These carbonate breccias thicken toward the west and show an angular discordance of about 15° with the underlying Triassic dolostones and Agnelli limestone. At Piz Bardella the Triassic dolostones and Agnelli limestone are tilted to the east with an angle between 22° and 43°. It is also important to note that the syntectonic sediments show major lateral changes in the composition of the clasts. While at Fuorcla Cotschna the breccias are dominated by footwall as well as hanging wall derived clasts, at Piz Bardella the breccias contain only hanging wall derived dolostone clasts (for more detail see Masini et al., 2011, and reference therein). The syntectonic sedimentary sequence grades conformably upward into the postrift sediments that contain strongly folded red cherts and shales of the Radiolarian Chert Fm.

4.3. The Southern Segment

The southern segment of the Middle Err unit, around Piz Rocabella, Piz d'Emmat Dadora, and Grevasalvas, is the most affected by Alpine reactivation. It corresponds to a stacking of different subunits that preserve internally pre-Alpine rift-related contacts (Epin et al., 2017). Between Piz Bardella and Piz d'Emmat Dadora (Figures 2 and 5), there is a remnant of a Jurassic detachment that can be correlated across the valley with the Jenatsch detachment flooring the Bardella block (blue line). The detachment surface is marked by the diagnostic, silica-rich green cataclasites. Black indurated gouges can also be observed locally. The detachment surface overlies granitic basement and a Permian volcano-sedimentary sequence (see subunit 1 on section Figure 5b). The detachment surface is overlain structurally by olistoliths of dolostones (maximum 30 m) that are overlain depositionally by Radiolarian Cherts, Calpionella, and Aptychus limestones Fm. forming the postrift sequence. Piz Rocabella is the only place in the Err nappe where postrift sediments directly overlie exhumed basement with a depositional contact. In a subunit overlying this unit (i.e., derived from further eastward; subunits 3 and 4 on Figure 5b) and located between Grevasalvas and Piz d'Emmat Dadora, another piece of the Jenatsch detachment fault is preserved. The footwall is made of granite and gneiss, and the detachment surface is made of green cataclasites. The hanging wall is made of syntectonic sedimentary breccias that consist of reworked dolostones that belong to the Bardella Fm. and grade up section into Saluver type sediments and postrift sediments.

4.4. North-South Correlations (Strike Section)

A comparison of the Jurassic structures preserved in the different segments in the Middle Err unit shows important along-strike variations of the detachment system. The Jurassic rift structures observed along a

north-south section shown in Figure 6 are within one and the same Alpine tectonic unit. The Middle Err unit is little affected, except at its northern and southern extremities, by Alpine reactivation. The main Alpine structures are third-order D1 structures and D3 folds (Figure 6).

The north-south section shown in Figure 6 shows the distribution and cross-cutting relationships between the three detachment faults presented before. In the northern part (Figure 6) a subhorizontal detachment fault can be found at an altitude of 3,000 m. It can be mapped from Piz d'Err to Piz Caldera to Piz Picuogl. This corresponds to the Jenatsch detachment fault (blue line, Figure 6). South of Piz Picuogl, this detachment fault plunges toward the south under Piz d'Agnel. In the lateral continuity, it reappears further south under Piz Bardella and Piz d'Emmat Dadora. Westward thrusting of the Piz Bardella along a thrust that reactivates the former detachment fault explains the repetition of the detachment fault in the section (Figure 6c). Along the north-south directed section, the Jenatsch detachment was structurally overlain by basement (gneiss and schists) in the north. In the central part it is overlain by the volcano-sedimentary Permian section and further south directly by postrift sediments. The footwall is made of granite in the southern and northern parts of the section, while in the central part of the section it is truncated/reactivated by an Alpine D1 thrust fault. Thus, where the Jenatsch detachment hits the edges of the Permian basin (at Piz d'Agnel in the north and Piz d'Emmat Dadora in the south; black line, Figures 2 and 6) it forms lateral ramps, that is, the detachment dip is perpendicular to the transport direction. This suggests that the lateral ramps of the Jenatsch detachment were controlled by the boundaries of the Permian basin and that the Permian basin was inverted during Jurassic extension. The east-west directed strike of the lateral ramp is compatible with the transport direction determined within the fault rocks of the Jurassic detachment system.

The Err detachment fault (green line, Figure 6) is only visible on the most northern part of the section. In north-south sections further east, it can be traced further southward due to the fact that it becomes the dominant structure east of the breakaway of the Jenatsch detachment at Piz Jenatsch. The base of the Err detachment is cross cut by the same D1 thrust fault that also truncates the Jenatsch detachment further to the west.

The third detachment described in this paper, the Agnel detachment, is only visible at Piz d'Agnel on the north-south directed section, where the Jenatsch detachment inverted the Permian basin (Figure 6). Its footwall is made of the Permian volcano-sedimentary sequence. Its hanging wall is only observable at Piz d'Agnel, where it is made of gneiss.

5. Detachment Structures in the Lower Err and Upper Platta Units

The Lower Err and Upper Platta units preserve relics of a former transition from exhumed continental to mantle rocks, similar to the Tasna nappe (Florineth & Froitzheim, 1994; Froitzheim & Rubatto, 1998; Manatschal et al., 2006). While these units are omitted along an Alpine D2 normal fault in the southern part of the study area, north of Piz Calderas these units are well preserved (Figures 2 and 7). The Lower Err unit is made in this area of porphyric granite that shows toward its top brittle anastomosing fault zones comprising characteristic silica-rich green cataclasites and black indurated gouges that are diagnostic for the extensional detachment faults (Manatschal, 1995, 1999). To the southeast (Figure 7b), the detachment is depositionally overlain by polymictic crystalline and carbonate sedimentary breccias. Further to the northwest, the detachment is structurally overlain by Permian volcanic rocks and Triassic dolostones (location of the detachment shown by the red line in Figure 7). Thus, the detachment fault was locally exhumed at the seafloor and directly overlain by syntectonic sedimentary breccias (southeast), while further to the northwest it is covered by a small allochthonous block (see section Figure 7b and schematic restoration Figure 7c). Further to the northwest, the detachment overlies exhumed mantle and is structurally overlain by a continent-derived basement that is strongly deformed and locally injected by syntectonic sediments.

6. Discussion

6.1. Three-Dimensional Restoration of an Extensional Detachment System

A detailed analysis of the detachment system exposed in the Err nappe allows proposing a 3-D model of its pre-Alpine architecture in the former hyperextended margin. In Figures 8a and 8b, we present a simplified 3-D restoration of the area shown in the map in Figure 2. The general extensional direction along the

detachment system is E-W, with the eastern part corresponding to the continentward part and the western part corresponding to the oceanward part.

The extreme western part (exposed in the northwest of the studied area between Castalegns and Parsettens, north of Piz d'Err, Figures 2, 7, and 8b) is characterized by the exhumation of the subcontinental mantle (i.e., the Upper Platta unit). This exhumation is due to the action of the red and violet detachment faults (Figure 8), referred to as the Agnel and the Upper Platta detachment faults, respectively. The footwall of the Agnel and Upper Platta detachment faults is made of granite on its continentward side and subcontinental mantle on its oceanward side (Figure 7). We interpret these detachment faults to be the first to exhume subcontinental mantle at the seafloor and consequently also the petrologic Moho, which is reactivated by a third-order D1 Alpine thrust that defines the present-day contact between the Lower Err unit and the Upper Platta unit (Figure 2).

In the northern segment, only the footwall of the Agnel detachment (red, Figure 8a) is visible, forming the top of the Piz Calderas (Figure 3). In the central segment, the Agnel detachment fault is preserved at Piz d'Agnel and its footwall built the Piz d'Agnel-Piz Neir ridge, composed of gneiss, granite, and a volcano-sedimentary sequence belonging to the Permian Neir basin. In the southern segment, direct evidence of the Agnel detachment fault does not exist; the Agnel detachment fault seems to disappear. However, at Piz Rocabella and Piz d'Emmat Dadora, an exhumation fault separates tectonized granitic and gneissic basement from the postrift sediments deposited on top of this exhumation fault. We propose that the southward termination of the extensional allochthon observed at Piz Bardella and the drastic thinning of the syntectonic sediments may be explained, as discussed below, by the interaction of the Agnel and Jenatsch detachment faults.

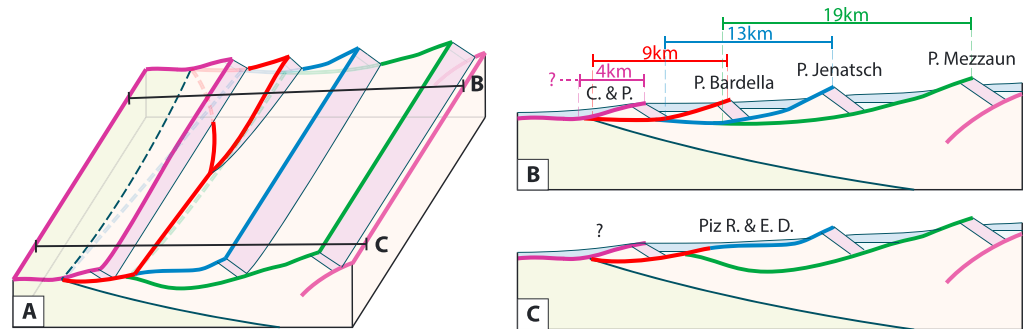
The Jenatsch detachment (blue, Figure 8) lies in the footwall of the Agnel detachment and is intersected by the latter. The Jenatsch detachment shows a lateral complexity (Figure 6) with the occurrence of a lateral ramp. This ramp coincides with a change in the composition of the basement from granitic and gneissic in the north to a volcano-sedimentary sequences to the south. Therefore, we interpret that the ramp may be controlled by the occurrence of the Permian Neir basin. The entire hanging wall of the Jenatsch detachment is tilted to the east and preserves a complete stratigraphic section including a Permo-Triassic section made of a thick volcano-sedimentary sequence and dolostones, stratigraphically overlain by evaporites of Carnian age, and massive dolostones and limestones of Upper Triassic to Lower Jurassic age. This hanging wall block, which can be mapped from the north toward Piz Bardella (Figures 2–4), abruptly terminates in the Julier valley. Since the footwall of the Jenatsch detachment continues south of the Julier valley together with remnants of the hanging wall block and synrift sediments, the lateral termination of the block cannot be explained by Alpine tectonics. We propose therefore that the southern termination of the Bardella extensional allochthon and the occurrence of a basement high at Piz Rocabella (see discussion above) can be best explained if the Jenatsch detachment and its hanging wall block are incised by the Agnel detachment. As a consequence, the southward termination of the allochthonous block is explained with an incisement of the Agnel detachment (see Davis & Lister, 1988, for examples of incisement and excisement structures). With this interpretation, we explain that the basement at Piz Rocabella is capped by detachment surfaces that are overlain by postrift sediments, explaining the dome-like structure, comparable to metamorphic core complexes or oceanic core complexes.

The Err detachment (green Figure 8) corresponds to the most continent ward detachment in the 3-D block (Figure 8). It is structurally overlain by small allochthonous blocks made of basement and Upper Triassic dolostones (e.g., Piz Laviner area), which are in contrast to the breakaway blocks (e.g., Bardella block) that are much smaller and do not represent the breakaway of a new detachment fault. Since in these blocks subevaporite levels (basement) are juxtaposed by younger lithologies (Upper Triassic) along decoupling levels that are in turn truncated by the detachment fault, we interpret these structures as resulting from the presence of salt tectonics (for further discussion see section 6.3.1.).

6.2. The Rolling Hinge Model in Hyperextended Domains

At a first order, the field observations show an in-sequence evolution of the detachment faults getting younger and shorter oceanward. These observations are schematically shown in Figure 9. The dip length of each detachment fault is shown in Figure 9b; the values represent minimum estimations. Note,

Insequence evolution, crosscutting relationships, and termination of allochthon block



Influence of Permian structures on detachment faults

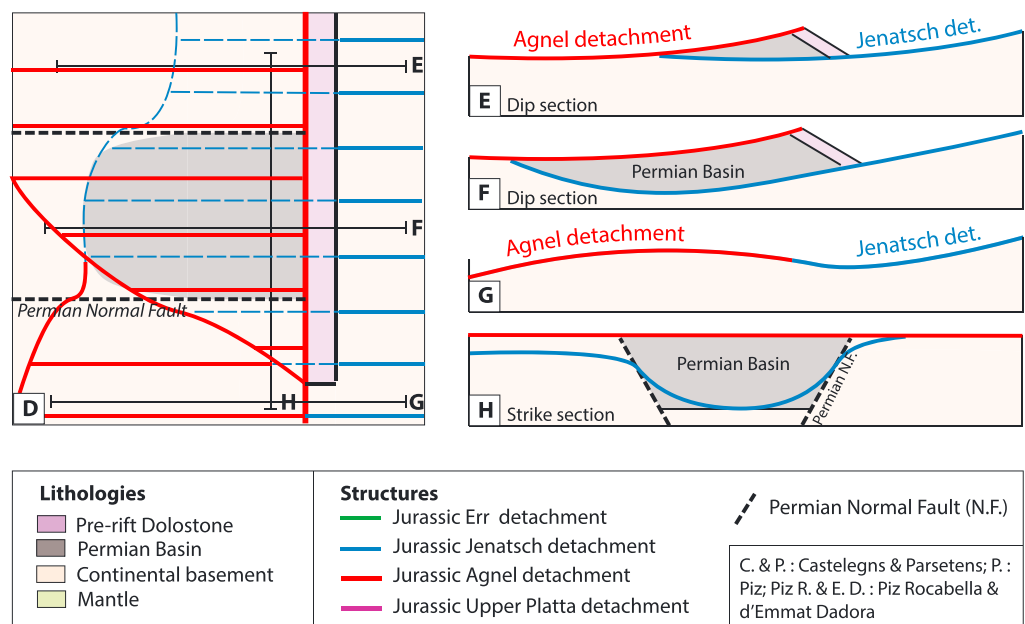


Figure 9. (a) Schematic 3-D block representing the lateral extend of allochthon blocks due to the interactions between the Agnel detachment (in red) and the Jenatsch detachment (in blue). (b and c) Sections illustrating the lateral variability of sections and the lateral termination of allochthonous block as observed across the Julier valley (see text for discussion). Figure 9b shows the estimated minimal values of the in dip length of the detachment faults. (d) Schematic map view of the Permian basin and its influence on the detachment faults (see sections E, F, G and H). (e–h) Sections showing the influence of a preexisting Permian basin on the detachment faults in deep and strike view.

however, that the geometry of detachment faults show important changes along strike. The distance shown in Figure 9b is measured on the map between a breakaway block (initiation of a detachment fault) and the intersection point between two detachment faults (dip termination of a detachment fault). The breakaway block of the Err detachment fault is not visible in the map in Figure 2 but on the map shown in Figure 1a it is located close to P. Mezzaun in the Engadin valley. The other breakaway points are not directly exposed but are projected and correspond to the intersection of a detachment fault and the continentward rotated prerift sequence.

These overall observations reported from the Err detachment system are, at the first order, compatible with the rolling hinge model proposed by observations made in the Basin and Range (Buck, 1988; Spencer, 1984; Wernicke, 1985; Wernicke & Axen, 1988) or exemplified in present-day distal rifted margins (Nirrengarten et al., 2016; Ranero & Pérez-Gussinyé, 2010). In the classical rolling hinge model (Buck, 1988; Figure 10), the propagation of the deformation evolves in sequence with the upward propagation of a new fault from the intersection point through the hanging wall. The upward propagation of a new fault that is rooting in

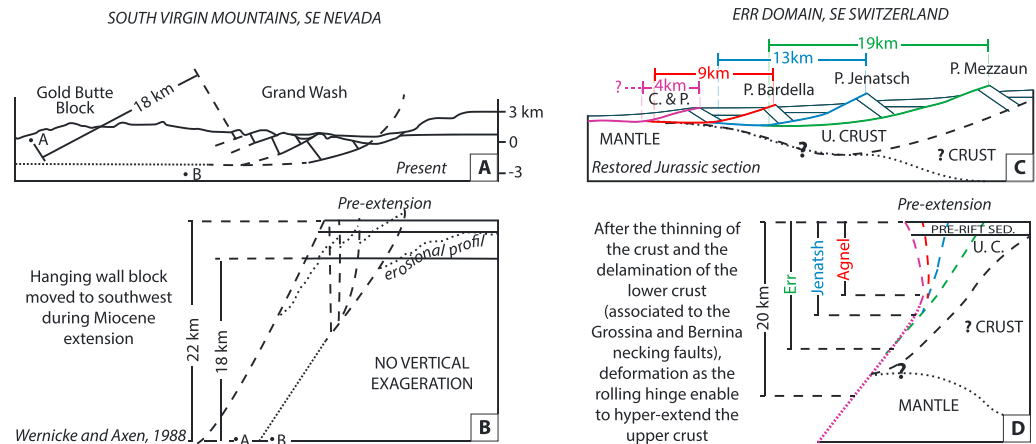


Figure 10. The rolling hinge model in a post orogenic collapse compared to a magma-poor, hyperextended rift system. (a and b) Example of the rolling hinge model expressed in a post orogenic collapse through the Virgin mountains, balanced and reconstructed cross sections from Wernicke & Axen, 1988 modified from Longwell 1945. (c and d) Example of the Err domain with balanced and reconstructed cross sections. C. & P. = Castelegns & Parsetens; P. = Piz; U.C. = Upper Crust.

the deeper active part of the existing fault creates a new allochthone block that is getting delaminated from the hanging wall and becomes part of the footwall. The creation of an allochthone block is assumed to occur because the old fault has been flexure and rotated to an angle too low to be able the accommodated further slip. The angular relationship between the new fault and the old fault at the intersection point are expected to be in the order of 20° to 30° (20° in the case of serpentines; Reston et al., 2007), which is compatible with the observations made in the Err nappe between the Err and the Jenatsch detachment faults.

In detail, however, the observations made in the Err nappe show that the geometrical relationships are more complex and controlled by inheritance. Field observations show that the detachment faults intersect each other with an in-sequence evolution, except for the Rocabella-Piz d'Emmat Darora area, where the relationship between detachment faults (Agnel and Jenatsch detachment faults) is more complex and an incisement can be observed (Figure 9; e.g., Davis and Lister, 1988). However, the major problem is that we do not have access to deeper parts of the detachment system in the Err nappe. We can therefore not say if the detachment faults rooted at depth in one major detachment fault as suggested by the rolling hinge model. The only information we have from the deeper part of the detachment system is indirect. For instance, we never found mylonites and middle or lower crustal rocks associated with the detachment system in the Err nappe. This suggests that the observed faults were active in the brittle crust and that deeper structures had to exist to thin and exhume the deeper parts of the crust. Indeed, as proposed by Mohn et al. (2012) and Duret et al. (2016), the hyperextended domain developed into an upper crustal block (e.g., H-Block of Lavier & Manatschal, 2006), which was disconnected from the ductile part of the crust during the necking phase and the faults observed in the hyperextended part initiated only after the crust had already been thinned to less than 15 km. For the study area this is supported indirectly by the study of mantle derived fluids. Indeed, the study of Pinto et al. (2013, 2015) and Incerpi et al. (2017) suggested that the Err detachment system was connected to the mantle, as fluids with a mantle signature occur along the detachment faults. In their interpretation, the Err detachment fault is the first detachment fault that penetrated into the mantle.

6.3. Importance of Inherited Structures

Detail mapping of the Err nappe enabled to show a complex 3-D architecture of the Jurassic detachment system and its hanging wall blocks. Two major factors seem to control the architecture of the detachment system and the architecture of the breakaway blocks: (1) inherited structures in the basement and (2) weak, low frictional layers (evaporites) in the prerift sedimentary succession.

6.3.1. Inherited Basement Structures Controlling the Architecture of Detachment Faults

The major inherited structure in the basement of the Err nappe corresponds to Permian normal faults bounding the Permian Neir basin (see Figures 2, 8, and 9). Examples of Permian basins strongly influencing the

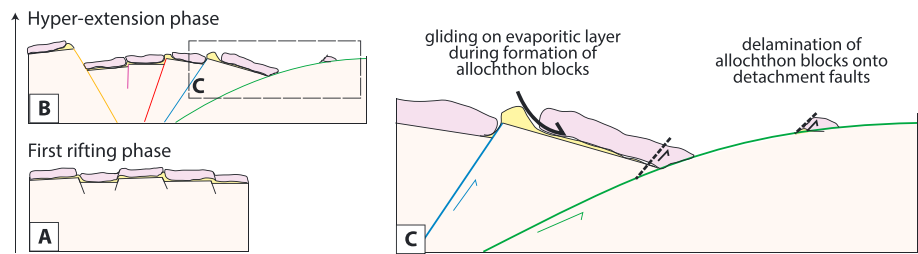


Figure 11. Influence of weak layers. (a and b) Show first-order structural evolution between the first rifting stage and the hyperextended phase, focusing on the cover movement. The observations suggest a strong link between evaporite tectonics (gravitational gliding) during the formation of the detachment faults. (c) Gravitational gliding over evaporate layers of the perift dolostone during the formation of allochthonous blocks occurring simultaneous with the exhumation along detachment faults.

subsequent deformation events have been described from the inverted Permian Verrucano basins in the Helvetic nappes (Pfiffner, 2014, *Geology of the Alps*, Figures 2–21). In the Err nappe, the existence of a Permian basin had a control on the evolution of the Jurassic detachment system. We previously described the lateral ramp of the Jenatsch detachment and discussed its interference with the preexisting Permian normal fault. The Jenatsch detachment inverted the Neir basin; however, the bounding normal faults were too steep to be reactivated completely (Figure 9H). As a consequence, the breakaway of the Permian normal faults have not been reactivated and they are preserved in the Piz d’Agnel-Corn Suvretta area (see Figure 6c). The lateral ramp of the Jenatsch detachment is consequently controlled by the Permian Neir basin (Figures 6, 8, and 9). The existence of this lateral ramp and its E-W directed strike shows that the transport direction along the Jenatsch detachment had to be E-W directed and parallel to the fault bounding the Neir basin. Although less well exposed, the southern termination of the Permian basin can be observed also south of the Julier valley in the area of Piz Rocabella and Piz d’Emmat Dadora. The southern termination of the Permian basin corresponds to the location where the Agnel detachment fault back steps and incises into the Jenatsch detachment resulting in the lateral termination of the break way block separating the two detachment faults (Figure 9). Thus, inherited structures can control lateral changes of the detachment fault geometry and result in modifications of the classical rolling hinge model.

6.3.2. Crosscutting Relationships and Termination of Allochthon Block

In the southern segment, the east-west striking Permian normal fault was truncated by the Jenatsch detachment fault. This coincides with the location where the hanging wall block separating the Agnel and Jenatsch detachment terminates. Thus, the interference of these two detachment faults at the southern termination of the Permian basin may explain the abrupt termination of the block exposed at Piz Bardella and the occurrence of a basement high capped by detachment faults at Piz Rocabella across the Julier valley (Figures 9). Indeed, we explain the lateral termination of the Bardella block as a consequence of the Agnel detachment fault that incised and truncated the Jenatsch detachment (see Figure 9). In other words, the Julier valley marks the area where a breakaway allochthon block separating two detachment faults to the north (the Agnel and Jenatsch detachment faults) changes to a basement high that is capped by two detachment faults, the Jenatsch detachment in the east that is truncated by the Agnel detachment on its oceanward side and stratigraphically covered by postrift sediments. This topographic high corresponds to a dome like structure comparable to metamorphic core complex or oceanic core complex (see Figure 14 in Reston & Ranero, 2011).

6.3.3. Inherited Weak Layers in the Perift Sediments Controlling Hanging Wall Structures

The role of *weak* layers, that is, of Triassic evaporites, during the formation of extensional allochthons is best observed at Piz Neir-Piz Bardella in the central segment of the Err nappe and along the Err detachment in the northern segment. Piz Neir and Piz Bardella present a succession of Permian volcano-sedimentary rocks and perift sediments. As shown in the section in Figure 4e, the Permian volcano-sedimentary sequence is separated from Upper Triassic dolostones and Lower Jurassic limestones along evaporites made of carnageules (evaporate residue) of Carnian age. The Permo-Triassic section is tilted at present to the east to 30°–50°, while the basal Jenatsch detachment is still subhorizontal. In the section in Figure 4e it can be seen that the dolostones overlying the evaporitic layer and forming the Piz Bardella are offset relative to the Permian volcano-sedimentary succession present at Piz Neir. We interpret this offset as the result of gravitational gliding associated to tilting and transfer of movement from the Jenatsch to the Agnel detachment (see

Figures 8e and 10). The gliding of the Upper Triassic dolostones over the evaporitic layer can explain the complex structures of the top of the block and the occurrence of rafted blocks overlying the detachment faults (Figure 11). Indeed, in the blocks overlying the detachment (e.g., Err detachment at Piz Lavinèr-Piz Bial), the preevaporite and postevaporite sequences are decoupled and never form a complete stratigraphic section. In the field, no evidence of syngravitational deformation is visible in the syntectonic and posttectonic sediments, which is consistent with these movements occurring during the early stage of the formation of the detachment blocks over the detachment faults. Moreover, during Alpine reactivation, the weak evaporite layers have been in many places reactivated as thrusts, making the final structure even more complex (for Alpine overprint see discussion in Epin et al., 2017, see their Figures 4 and 5).

7. Conclusion

The Err nappe preserves remnants of a well preserved detachment system that formed in a hyperextended domain of a magma-poor rifted margin. It is at present the best place to study, in the field, the 3-D architecture and evolution of a detachment system in a hyperextended rift context. In this paper, we present maps and sections that describe the 3-D architecture of this Err detachment system. The Err detachment system is made of several detachment faults evolving in sequence to mantle exhumation. Our observations show important 3-D variations associated to inherited structures, which seem to favor the lateral termination of allochthonous blocks associated to a hyperextended rifting system. Indeed we identify at least four detachment faults evolving in sequence to forming the hyperextended domain and leading to exhumation of the subcontinental mantle. The length of the faults decreases oceanward, associated to the decreasing size of the breakaway blocks. We show that the architecture of the detachment structures and of the structurally overlying breakaway blocks is strongly controlled by inherited structures, which correspond to a Permian basin and a prerift evaporitic layer. The lateral variability of detachment faults (e.g., lateral ramps) are strongly influenced by preexisting structures such as the Permian basin in the case of this study. The results of this study enable to explain, based on field observations, the detailed evolution of a detachment system that is related to hyperextension and exhumation of mantle in the most distal part of a rifted margin.

Acknowledgments

The authors are grateful to the financial support of Total supporting the PhD of the first author. We would also like to thank the numerous colleagues from academia and industry that participated in field excursions through the study area and contributed in a constructive way to the work that we present in this paper. We particularly thank the reviewers Adrian Pfiffner, Gary Axen, and Tim Reston and the Associate Editor Ernst Willingshofer for the very constructive reviews. All the data used are available within figures and are listed in the references.

References

- Axen, G. J., & Bartley, J. M. (1997). Field tests of rolling hinges: Existence, mechanical types, and implications for extensional tectonics. *Journal of Geophysical Research*, 102(B9), 20,515–20,537. <https://doi.org/10.1029/97JB01355>
- Beltrando, M., Manatschal, G., Mohn, G., Dal Piaz, G. V., Brovarone, A. V., & Masini, E. (2014). Recognizing remnants of magma-poor rifted margins in high-pressure orogenic belts: The Alpine case study. *Earth-Science Reviews*, 131, 88–115. <https://doi.org/10.1016/j.earscirev.2014.01.001>
- Bernoulli, D. (1964). Zur Geologie des Monte Generoso (Lombardische Alpen): ein Beitrag zur Kenntnis der süd-alpinen Sedimente. *na*.
- Bill, M., O'Dogherty, L., Guex, J., Baumgartner, P. O., & Masson, H. (2001). Radiolarite ages in Alpine-Mediterranean ophiolites: Constraints on the oceanic spreading and the Tethys-Atlantic connection. *Geological Society of America Bulletin*, 113(1), 129–143. [https://doi.org/10.1130/0016-7606\(2001\)113<0129:RAIAMO>2.0.CO;2](https://doi.org/10.1130/0016-7606(2001)113<0129:RAIAMO>2.0.CO;2)
- Boillot, G., Recq, M., Winterer, E., Meyer, A., Applegate, J., Baltuck, M., et al. (1987). Tectonic denudation of the upper mantle along passive margins: A model based on drilling results (ODP leg 103, western Galicia margin, Spain). *Tectonophysics*, 132(4), 335–342. [https://doi.org/10.1016/0040-1951\(87\)90352-0](https://doi.org/10.1016/0040-1951(87)90352-0)
- Boillot, G., Winterer, E. L., Meyer, A. W., Applegate, J., Baltuck, M., Bergen, J. A., et al. (1988). *Proceedings of the Ocean Drilling Program, Scientific results, Galicia margin; covering Leg 103 of the cruises of the drilling vessel JOIDES Resolution, Ponta Delgada, Azores, to Bremerhaven, Germany, 25 April 1985-19 June 1985*. College Station, TX: Texas A & M University, Ocean Drilling Program, College Station, TX.
- Brune, S., Heine, C., Pérez-Gussinyé, M., & Sobolev, S. V. (2014). Rift migration explains continental margin asymmetry and crustal hyperextension. *Nature Communications*, 5(1), 4014. <https://doi.org/10.1038/ncomms5014>
- Buck, W. R. (1988). Flexural rotation of normal faults. *Tectonics*, 7(5), 959–973. <https://doi.org/10.1029/TC007i005p00959>
- Butler, R. (1989). The influence of pre-existing basin structure on thrust system evolution in the Western Alps. *Geological Society, London, Special Publications*, 44(1), 105–122. <https://doi.org/10.1144/GSL.SP.1989.044.01.07>
- Butler, R. W. H., Tavarnelli, E., & Grasso, M. (2006). Structural inheritance in mountain belts: An Alpine–Apennine perspective. *Journal of Structural Geology*, 28(11), 1893–1908. <https://doi.org/10.1016/j.jsg.2006.09.006>
- Cornelius, H. (1932). Geologische Karte der Err-Julier-Gruppe 1: 25000. Schweizerische Geologische Kommission Spezialkarte, 115.
- Davis, G. A., Anderson, J. L., Frost, E. G., & Shackelford, T. J. (1980). Mylonitization and detachment faulting in the Whipple-Buckskin-Rawhide Mountains terrane, southeastern California and western Arizona. *Geological Society of America Memoirs*, 153, 79–130. <https://doi.org/10.1130/MEM153-p79>
- Davis, G. A., & Lister, G. (1988). Detachment faulting in continental extension; perspectives from the southwestern US Cordillera. *Geological Society of America Special Papers*, 218, 133–160. <https://doi.org/10.1130/SPE218-p133>
- Decarlis, A., Manatschal, G., Hauptert, I., & Masini, E. (2015). The tectono-stratigraphic evolution of distal, hyper-extended magma-poor conjugate rifted margins: Examples from the Alpine Tethys and Newfoundland–Iberia. *Marine and Petroleum Geology*, 68, 54–72. <https://doi.org/10.1016/j.marpetgeo.2015.08.005>
- Doessegger, R. (1974). Verrucano und "Buntsandstein" in den Unterengadiner Dolomiten. Diss. Naturwiss. ETH Zürich, Nr. 5346, 0000. Ref.: Trümpy, R.; Korref.: Gansser, A.

- Dommergues, J.-L., Meister, C., & Manatschal, G. (2012). Early Jurassic ammonites from Bivio (Lower Austroalpine unit) and Ardez (Middle Penninic unit) areas: A biostratigraphic tool to date the rifting in the Eastern Swiss Alps. *Revue de Paléobiologie*, 31, 43–52.
- Duret, T., Petri, B., Mohn, G., Schmalholz, S., Schenker, F., & Müntener, O. (2016). The importance of structural softening for the evolution and architecture of passive margins. *Scientific Reports*, 6(1). <https://doi.org/10.1038/srep38704>
- Elter, P. (1972). La zona ofiolitífera del Bracco nel quadro dell'Appennino Settentrionale. *Introduzione alla geologia delle Liguridi*, 66, 5–35.
- Epin, M.-E., Manatschal, G., & Amann, M. (2017). Defining diagnostic criteria to describe the role of rift inheritance in collisional orogens: The case of the Err-Platta nappes (Switzerland). *Swiss Journal of Geosciences*, 110(2), 419–438. <https://doi.org/10.1007/s00015-017-0271-6>
- Ferreiro Mählmann, R. (1994). Zur Bestimmung von Diagenesehöhe und beginnender Metamorphose: Temperaturgeschichte und Tektogenese des Austroalpins und Südpenninikums in Vorarlberg und Mittelbünden. Institut für Geochemie, *Petrologie und Lagerstättenkunde der Johann Wolfgang Goethe Universität*.
- Ferreiro Mählmann, R. (1996). The pattern of diagenesis and metamorphism by vitrinite reflectance and illite-'crystallinity' in Mittelbünden and in the Oberhalbstein. Part 2: Correlation of coal petrographical and of mineralogical parameters. *Schweizerische Mineralogische und Petrographische Mitteilungen*, 76, 23–46.
- Finger, W. (1978). Die Zone von Sameden (Unterostalpine Decken, Graubünden) und ihre Jurassischen Brekzien. *Mitteilungen aus dem Geologischen Institut ETH und Universität Zuerich*, NF224, 1–140.
- Florineth, D., & Froitzheim, N. (1994). Transition from continental to oceanic basement in the Tasna nappe (Engadine window, Graubünden, Switzerland)—Evidence for early cretaceous opening of the Valais Ocean. *Schweizerische Mineralogische und Petrographische Mitteilungen*, 74(3), 437–448.
- Froitzheim, N., & Eberli, G. P. (1990). Extensional detachment faulting in the evolution of a Tethys passive continental margin, Eastern Alps, Switzerland. *Geological Society of America Bulletin*, 102(9), 1297–1308. [https://doi.org/10.1130/0016-7606\(1990\)102<1297:EDFITE>2.3.CO;2](https://doi.org/10.1130/0016-7606(1990)102<1297:EDFITE>2.3.CO;2)
- Froitzheim, N., & Manatschal, G. (1996). Kinematics of Jurassic rifting, mantle exhumation, and passive-margin formation in the Austroalpine and Penninic nappes (eastern Switzerland). *Geological Society of America Bulletin*, 108(9), 1120–1133. [https://doi.org/10.1130/0016-7606\(1996\)108<1120:KOJRM>2.3.CO;2](https://doi.org/10.1130/0016-7606(1996)108<1120:KOJRM>2.3.CO;2)
- Froitzheim, N., & Rubatto, D. (1998). Continental breakup by detachment faulting: Field evidence and geochronological constraints (Tasna nappe, Switzerland). *Terra Nova*, 10(4), 171–176. <https://doi.org/10.1046/j.1365-3121.1998.00187.x>
- Froitzheim, N., Schmid, S. M., & Conti, P. (1994). Repeated change from crustal shortening to orogen-parallel extension in the Austroalpine units of Graubünden. *Eclogae Geologicae Helveticae*, 87(2), 559–612.
- Handy, M. (1996). The transition from passive to active margin tectonics: A case study from the Zone of Samedan (eastern Switzerland). *Geologische Rundschau*, 85(4), 832–851. <https://doi.org/10.1007/BF02440114>
- Handy, M., Herwegh, M., & Regli, C. (1993). Tektonische Entwicklung der westlichen Zone von Samedan (Oberhalbstein, Graubünden, Schweiz). *Eclogae Geologicae Helveticae*, 86(3), 785–817.
- Handy, M. R., Herwegh, M., Kamber, B., Tietz, R., & Villa, I. (1996). Geochronologic, petrologic and kinematic constraints on the evolution of the Err-Platta boundary, part of a fossil continent-ocean suture in the Alps (eastern Switzerland). *Schweizerische Mineralogische und Petrographische Mitteilungen*, 76(3), 453–474.
- Huisman, R., & Beaumont, C. (2011). Depth-dependent extension, two-stage breakup and cratonic underplating at rifted margins. *Nature*, 473(7345), 74–78. <https://doi.org/10.1038/nature09988>
- Incerpi, N., Martire, L., Manatschal, G., & Bernasconi, S. M. (2017). Evidence of hydrothermal fluid flow in a hyperextended rifted margin: the case study of the Err nappe (SE Switzerland). *Swiss Journal of Geosciences*, 1–18.
- John, B. E. (1987). Geometry and evolution of a mid-crustal extensional fault system: Chemehuevi Mountains, southeastern California. *Geological Society, London, Special Publications*, 28(1), 313–335. <https://doi.org/10.1144/GSL.SP.1987.028.01.20>
- John, B. E., & Cheadle, M. J. (2010). Deformation and alteration associated with oceanic and continental detachment fault systems: Are they similar. Diversity of Hydrothermal Systems on Slow Spreading Ocean Ridges, *Geophysical Monograph Series*, 188, 175–206. <https://doi.org/10.1029/2008GM000772>
- John, B. E., & Foster, D. A. (1993). Structural and thermal constraints on the initiation angle of detachment faulting in the southern Basin and Range: The Chemehuevi Mountains case study. *Geological Society of America Bulletin*, 105(8), 1091–1108. [https://doi.org/10.1130/0016-7606\(1993\)105<1091:SATCOT>2.3.CO;2](https://doi.org/10.1130/0016-7606(1993)105<1091:SATCOT>2.3.CO;2)
- Lagabrielle, Y., & Cannat, M. (1990). Alpine Jurassic ophiolites resemble the modern central Atlantic basement. *Geology*, 18(4), 319–322. [https://doi.org/10.1130/0091-7613\(1990\)018<0319:AJORTM>2.3.CO;2](https://doi.org/10.1130/0091-7613(1990)018<0319:AJORTM>2.3.CO;2)
- Lavier, L. L., & Manatschal, G. (2006). A mechanism to thin the continental lithosphere at magma-poor margins. *Nature*, 440(7082), 324–328. <https://doi.org/10.1038/nature04608>
- Lemoine, M., Tricart, P., & Boillot, G. (1987). Ultramafic and gabbroic ocean floor of the Ligurian Tethys (Alps, Corsica, Apennines): In search of a genetic model. *Geology*, 15(7), 622–625. [https://doi.org/10.1130/0091-7613\(1987\)15<622:UAGOF>2.0.CO;2](https://doi.org/10.1130/0091-7613(1987)15<622:UAGOF>2.0.CO;2)
- Lister, G. S., & Davis, G. A. (1989). The origin of metamorphic core complexes and detachment faults formed during Tertiary continental extension in the northern Colorado River region, USA. *Journal of Structural Geology*, 11(1–2), 65–94. [https://doi.org/10.1016/0191-8141\(89\)90036-9](https://doi.org/10.1016/0191-8141(89)90036-9)
- Manatschal, G. (1995). *Jurassic rifting and formation of a passive continental margin (Platta and Err Nappes, Eastern Switzerland): Geometry, kinematics and geochemistry of fault rocks and a comparison with the Galicia margin*. (Doctoral dissertation, ETH Zurich) Eidgenössischen Technischen Hochschule Zürich. <https://doi.org/10.3929/ethz-a-001533748>
- Manatschal, G. (1999). Fluid- and reaction-assisted low-angle normal faulting: Evidence from rift-related brittle fault rocks in the Alps (Err Nappe, eastern Switzerland). *Journal of Structural Geology*, 21(7), 777–793. [https://doi.org/10.1016/S0191-8141\(99\)00069-3](https://doi.org/10.1016/S0191-8141(99)00069-3)
- Manatschal, G. (2004). New models for evolution of magma-poor rifted margins based on a review of data and concepts from West Iberia and the Alps. *International Journal of Earth Sciences*, 93(3), 432–466.
- Manatschal, G., & Bernoulli, D. (1999). Architecture and tectonic evolution of nonvolcanic margins: Present-day Galicia and ancient Adria. *Tectonics*, 18(6), 1099–1119. <https://doi.org/10.1029/1999TC900041>
- Manatschal, G., Engström, A., Desmurs, L., Schaltegger, U., Cosca, M., Müntener, O., & Bernoulli, D. (2006). What is the tectono-metamorphic evolution of continental break-up: The example of the Tasna Ocean–Continent Transition. *Journal of Structural Geology*, 28(10), 1849–1869. <https://doi.org/10.1016/j.jsg.2006.07.014>
- Manatschal, G., Froitzheim, N., Rubenach, M., & Turrin, B. (2001). The role of detachment faulting in the formation of an ocean-continent transition: Insights from the Iberia Abyssal Plain. *Geological Society, London, Special Publications*, 187(1), 405–428. <https://doi.org/10.1144/GSL.SP.2001.187.01.20>
- Manatschal, G., Lavier, L., & Chenin, P. (2015). The role of inheritance in structuring hyperextended rift systems: Some considerations based on observations and numerical modeling. *Gondwana Research*, 27(1), 140–164. <https://doi.org/10.1016/j.gr.2014.08.006>

- Manatschal, G., Marquer, D., & Früh-Green, G. L. (2000). Channelized fluid flow and mass transfer along a rift-related detachment fault (Eastern Alps, southeast Switzerland). *Geological Society of America Bulletin*, 112(1), 21–33. [https://doi.org/10.1130/0016-7606\(2000\)112<21:CFAMT>2.0.CO;2](https://doi.org/10.1130/0016-7606(2000)112<21:CFAMT>2.0.CO;2)
- Manatschal, G., & Nievergelt, P. (1997). A continent-ocean transition recorded in the Err and Platta nappes (Eastern Switzerland). *Eclogae Geologicae Helveticae*, 90(1), 3–27.
- Masini, E., & Manatschal, G. (2014). The Err detachment in SE Switzerland: A witness of how continents break apart. *International Journal of Earth Sciences*, 103(1), 121–122. <https://doi.org/10.1007/s00531-013-0924-2>
- Masini, E., Manatschal, G., & Mohn, G. (2013). The Alpine Tethys rifted margins: Reconciling old and new ideas to understand the stratigraphic architecture of magma-poor rifted margins. *Sedimentology*, 60(1), 174–196. <https://doi.org/10.1111/sed.12017>
- Masini, E., Manatschal, G., Mohn, G., Ghiene, J. F., & Lafont, F. (2011). The tectono-sedimentary evolution of a supra-detachment rift basin at a deep-water magma-poor rifted margin: The example of the Samedan Basin preserved in the Err nappe in SE Switzerland. *Basin Research*, 23(6), 652–677. <https://doi.org/10.1111/j.1365-2117.2011.00509.x>
- Masini, E., Manatschal, G., Mohn, G., & Unternehr, P. (2012). Anatomy and tectono-sedimentary evolution of a rift-related detachment system: The example of the err detachment (central Alps, SE Switzerland). *Geological Society of America Bulletin*, 124(9–10), 1535–1551. <https://doi.org/10.1130/B30557.1>
- Mohn, G., Manatschal, G., Beltrando, M., & Hauptert, I. (2014). The role of rift-inherited hyper-extension in Alpine-type orogens. *Terra Nova*, 26(5), 347–353. <https://doi.org/10.1111/ter.12104>
- Mohn, G., Manatschal, G., Beltrando, M., Masini, E., & Kuszniir, N. (2012). Necking of continental crust in magma-poor rifted margins: Evidence from the fossil Alpine Tethys margins. *Tectonics*, 31, TC1012. <https://doi.org/10.1029/2011TC002961>
- Mohn, G., Manatschal, G., Masini, E., & Müntener, O. (2011). Rift-related inheritance in orogens: A case study from the Austroalpine nappes in Central Alps (SE-Switzerland and N-Italy). *International Journal of Earth Sciences*, 100(5), 937–961. <https://doi.org/10.1007/s00531-010-0630-2>
- Nagel, T. J., & Buck, W. R. (2007). Control of rheological stratification on rifting geometry: A symmetric model resolving the upper plate paradox. *International Journal of Earth Sciences*, 96(6), 1047–1057. <https://doi.org/10.1007/s00531-007-0195-x>
- Nirrengarten, M., Manatschal, G., Yuan, X. P., Kuszniir, N. J., & Maillot, B. (2016). Application of the critical Coulomb wedge theory to hyper-extended, magma-poor rifted margins. *Earth and Planetary Science Letters*, 442, 121–132. <https://doi.org/10.1016/j.epsl.2016.03.004>
- Pérez-Gussinye, M., & Reston, T. J. (2001). Rheological evolution during extension at nonvolcanic rifted margins: Onset of serpentinization and development of detachments leading to continental breakup (English). *Journal of Geophysical Research*, 106(B3), 3961–3975. <https://doi.org/10.1029/2000JB900325>
- Péron-Pinvidic, G., & Manatschal, G. (2010). From microcontinents to extensional allochthons: Witnesses of how continents rift and break apart? *Petroleum Geoscience*, 16(3), 189–197. <https://doi.org/10.1144/1354-079309-903>
- Péron-Pinvidic, G., Manatschal, G., Minchull, T. A., & Sawyer, D. S. (2007). Tectonosedimentary evolution of the deep Iberia-Newfoundland margins: Evidence for a complex breakup history. *Tectonics*, 26, TC2011. <https://doi.org/10.1029/2006TC001970>
- Pfiffner, O. A. (2014). *Geology of the Alps*. - Revised and updated translation of Geologie der Alpen, Second Edition, John Wiley & Sons, Limited, 392. ISBN 1118708113, 9781118708118.
- Picazo, S., Manatschal, G., Cannat, M., & Andréani, M. (2013). Deformation associated to exhumation of serpentinized mantle rocks in a fossil Ocean Continent Transition: The Totalp unit in SE Switzerland. *Lithos*, 175, 255–271.
- Pinto, V. H., Manatschal, G., Karpoff, A. M., Masini, E., Lemarchand, D., Hayman, N., & Viana, A. (2013). Fluid history in hyper-extended rifted margins: Examples from the fossil Alpine and western Pyrenean rift systems and the present-day Iberia rifted continental margin. Paper presented at the EGU General Assembly Conference Abstracts.
- Pinto, V. H. G., Manatschal, G., Karpoff, A. M., & Viana, A. (2015). Tracing mantle-reacted fluids in magma-poor rifted margins: The example of Alpine Tethyan rifted margins. *Geochemistry, Geophysics, Geosystems*, 16, 3271–3308. <https://doi.org/10.1002/2015GC005830>
- Ranero, C. R., & Pérez-Gussinyé, M. (2010). Sequential faulting explains the asymmetry and extension discrepancy of conjugate margins. *Nature*, 468(7321), 294–299. <https://doi.org/10.1038/nature09520>
- Reston, T. J., Gaw, V., Pennell, J., Klaeschen, D., Stubenrauch, A., & Walker, I. (2004). Extreme crustal thinning in the south Porcupine Basin and the nature of the Porcupine Median High: Implications for the formation of non-volcanic rifted margins. *Journal of the Geological Society*, 161(5), 783–798. <https://doi.org/10.1144/0016-764903-036>
- Reston, T. J., Leythäuser, T., Booth-Rea, G., Sawyer, D., Klaeschen, D., & Long, C. (2007). Movement along a low-angle normal fault: The S reflector west of Spain. *Geochemistry, Geophysics, Geosystems*, 8, Q06002. <https://doi.org/10.1029/2006GC001437>
- Reston, T. J., & McDermott, K. G. (2011). Successive detachment faults and mantle unroofing at magma-poor rifted margins. *Geology*, 39(11), 1071–1074. <https://doi.org/10.1130/G32428.1>
- Reston, T. J., & Ranero, C. R. (2011). The 3-D geometry of detachment faulting at mid-ocean ridges. *Geochemistry, Geophysics, Geosystems*, 12, Q0AG05. <https://doi.org/10.1029/2011GC003666>
- Schmid, S. M., Pfiffner, O.-A., Froitzheim, N., Schönborn, G., & Kissling, E. (1996). Geophysical-geological transect and tectonic evolution of the Swiss-Italian Alps. *Tectonics*, 15(5), 1036–1064. <https://doi.org/10.1029/96TC00433>
- Schmid, S. M., Fügenschuh, B., Kissling, E., & Schuster, R. (2004). Tectonic map and overall architecture of the Alpine orogen. *Eclogae Geologicae Helveticae*, 97(1), 93–117. <https://doi.org/10.1007/s00015-004-1113-x>
- Spencer, J. E. (1984). Role of tectonic denudation in warping and uplift of low-angle normal faults. *Geology*, 12(2), 95–98. [https://doi.org/10.1130/0091-7613\(1984\)12<95:ROTDIW>2.0.CO;2](https://doi.org/10.1130/0091-7613(1984)12<95:ROTDIW>2.0.CO;2)
- Spencer, J. E., & Chase, C. G. (1989). Role of crustal flexure in initiation of low-angle normal faults and implications for structural evolution of the Basin and Range province. *Journal of Geophysical Research*, 94(B2), 1765–1775. <https://doi.org/10.1029/JB094iB02p01765>
- Steinmann, G. (1925). Gibt es fossile Tiefseeablagerungen von erdgeschichtlicher Bedeutung? *Geologische Rundschau*, 16(6), 435–468. <https://doi.org/10.1007/BF01801627>
- Stöcklin, J. (1949). Zur Geologie der nördlichen Errgruppe Wischen Val d'Err und Weissenstein (Graubünden). PhD thesis, ETU Zurich.
- Sutra, E., & Manatschal, G. (2012). How does the continental crust thin in a hyperextended rifted margin? Insights from the Iberia margin. *Geology*, 40(2), 139–142. <https://doi.org/10.1130/G32786.1>
- Wernicke, B. (1985). Uniform-sense normal simple shear of the continental lithosphere. *Canadian Journal of Earth Sciences*, 22(1), 108–125. <https://doi.org/10.1139/e85-009>
- Wernicke, B., & Axen, G. J. (1988). On the role of isostasy in the evolution of normal fault systems. *Geology*, 16(9), 848–851. [https://doi.org/10.1130/0091-7613\(1988\)016<0848:OTROI>2.3.CO;2](https://doi.org/10.1130/0091-7613(1988)016<0848:OTROI>2.3.CO;2)
- Whitney, D. L., Teyssier, C., Rey, P., & Buck, W. R. (2013). Continental and oceanic core complexes. *Geological Society of America Bulletin*, 125(3–4), 273–298. <https://doi.org/10.1130/B30754.1>